ELSEVIER

Journal of Organometallic Chemistry 538 (1997) 223–239

Journal of Organometallic Chemistry

Hydrocarbyl derivatives of $[UCl_2\{HB(pz)_3\}_2]$: synthesis, characterization and reactivity studies towards protic substrates and ketones

M. Paula C. Campello [a], Maria José Calhorda [b,c], Ângela Domingos [a], Adelino Galvão [d], João Paulo Leal [a], A. Pires de Matos [a], Isabel Santos [a,*]

[a] *Departamento de Química, ITN, 2686 Sacavém Codex, Portugal*
[b] *I.T.Q.B., R. da Quinta Grande 6, Apt. 127, 2780 Oeiras, Portugal*
[c] *Faculdade de Ciências, Edifício C1, Campo Grande, 1700 Lisboa, Portugal*
[d] *Departamento de Engenharia Química, Instituto Superior Técnico, 1096 Lisboa Codex, Portugal*

Received 8 November 1996; revised 10 January 1997; accepted 16 January 1997

Abstract

The reaction of $[UCl_2\{HB(pz)_3\}_2]$ (**1**) with lithium alkyls LiR (R = Me, CH_2SiMe_3, C_6H_4-*o*-CH_2NMe_2) in the 1:1 or 1:2 molar ratio affords the compounds $[UClR\{HB(pz)_3\}_2]$ (pz = $C_3H_3N_2$, R = Me (**2**), CH_2SiMe_3 (**3**), C_6H_4-*o*-CH_2NMe_2 (**4**)) and $[UR_2\{HB(pz)_3\}_2]$ (R = Me (**5**), CH_2SiMe_3 (**6**)) respectively in 60–80% yield. Complex **2** can also be obtained (60% yield) by redistribution at room temperature between the complexes **1** and **5**. Compounds **2**, **3** and **4** react with pzH providing $[UCl(pz)\{HB(pz)_3\}_2]$ (**7**) in almost quantitative yield and **5** and **6** react also with pzH leading to $[U(pz)_2\{HB(pz)_3\}_2]$ (**8**). The alkoxide $[U(OC_6H_4$-*o*-$OMe)_2\{HB(pz)_3\}_2]$ (**9**) was synthesized by reacting **5** or **6** with guaiacol. By reacting the chlorohydrocarbyls **2**, **3** or **4** with excess of acetone the aldolate $[UCl(OCMe_2CH_2(C{=}O)Me)\{HB(pz)_3\}_2]$ (**11**) was obtained, due to the activation of α-CH bond of acetone; however, for **3** the reaction is not clean and a mixture of **11** and $[UCl(OCMe_2CH_2SiMe_3)\{HB(pz)_3\}_2]$ (**12**) is always obtained. Stoichiometric amounts of acetone insert into the metal–carbon bonds of **2** and **5** yielding $[UCl(O^tBu)\{HB(pz)_3\}_2]$ and $[U(O^tBu)_2\{HB(pz)_3\}_2]$ respectively, while the insertion product $[U(OCMe_2CH_2SiMe_3)_2\{HB(pz)_3\}_2]$ (**10**) can only be obtained when **6** reacts with excess of this substrate. **9** crystallizes from toluene/hexane in the triclinic space group $P\bar{1}$ with unit cell dimensions $a = 12.295(2)$ Å, $b = 12.640(2)$ Å, $c = 13.994(2)$ Å, $\alpha = 76.10(1)°$, $\beta = 72.50(1)°$, $\gamma = 80.71(1)°$, $V = 2004(2)$ Å^3 and $Z = 2$. Recrystallization of a mixture containing $[UCl(O^tBu)HB(pz)_{32}]$ and **11** led to a decomposition product which has been characterized by X-ray structural analysis as $[UCl(Hpz)(O^tBu)(\mu\text{-}O)B(\mu\text{-}pz)(pz)_2]_2$ (**13**): monoclinic $P2_1/n$, $a = 13.701(3)$ Å, $b = 11.337(2)$ Å, $c = 14.857(4)$ Å, $\beta = 104.65(2)°$, $V = 2233(1)$ Å^3 and $Z = 2$. Extended Hückel molecular orbital calculations provided some information on the bonding capabilities of the $[U\{HB(pz)_3\}_2]$ fragment compared to $[U(C_5Me_5)_2]$ and on the vulnerability of the poly(pyrazolyl)borate ligands to nucleophilic attack.

Keywords: Uranium; Poly(pyrazolyl)borates; Hydrocarbyl; Synthesis; Reactivity; Molecular orbital calculations

1. Introduction

Complexes of the type $[MX_2Cp_2]$ have played an important role in transition metal chemistry. Analogous compounds with the actinides are not stable and disproportion towards $[UClCp_3]$ and $[UCl_3Cp]$ was observed for uranium [1]. For thorium this process was prevented by using a bidentate phosphine, 1,2-bis(dimethylphosphino)ethane, which allowed the characterization of $[ThCl_2Cp_2(dmpe)]$ [2]. Stabilization against redistribution was also achieved by the use of bulky substituted cyclopentadienyls which in fact lead to stable complexes $[AnX_2Cp^*_2]$ (An = U, Th; $Cp^* = C_5Me_5$, C_5Me_4Et, C_5H_3-1,3$(SiMe_3)_2$, C_9H_7, C_4Me_4P; X = Cl or BH_4) [3–7]. Some other sterically demanding groups, different from cyclopentadienyls, were also used as supporting ligands and allowed the synthesis of the compounds $[UCl_2\{C_6H_5Co\{P(O)(OEt)_2\}_3\}_2]$ [8], $[UCl_2\{OC(^tBu)_3\}_2(thf)_2]$ [9] and $[ThBr_2(O\text{-}2,6\text{-}^tBu_2C_6H_3)_2]$ [10]. To see whether these complexes could be good precursors in the preparation of σ-hydrocarbyls and to study the reactivity of the metal–carbon bonds has been one of the main goals of this chemistry. So far, the cyclopentadienyl ligands are the ones which have played the most important role in the stabilization of σ-hydrocarbyls, and there is a great deal of

* Corresponding author.

PII S0022-328X(97)00078-8

organometallic chemistry associated with those complexes [5,11,12]. From this family of compounds we must refer to the pioneer work of Marks with $[AnCl_2(C_5Me_5)_2]$ (An = U, Th), and the large variety of bis(hydrocarbyl) and chlorohydrocarbyl complexes readily prepared from $[AnCl_2(C_5Me_5)_2]$ by metathesis reactions (Eq. (1)) [11]:

$$[AnCl_2(C_5Me_5)_2] + xLiR \xrightarrow[x=1 \text{ or } 2]{Et_2O} [AnR_xCl_{(2-x)}(C_5Me_5)_2] + xLiCl \quad (1)$$

The hydro(trispyrazolyl)borate, which has been compared to pentamethylcyclopentadienyl from the steric and electronic point of view [13,14], also allowed the stabilization of the complexes $[AnCl_2\{HB(pz)_3\}_2]$ [15], (An = U, Th) and from this precursor some σ-hydrocarbyls have been prepared [16,17]. To evaluate the effect of the hydro(trispyrazolyl)borate ligands on the stability and reactivity of U–C σ bonds was the main goal of this work. This paper describes the synthesis, characterization and some preliminary reactivity studies of [bishydrotris(pyrazolyl)borato] uranium hydrocarbyls. A portion of this work has been the subject of a previous communication [16].

2. Experimental

2.1. General procedures

The reactions were carried under an argon atmosphere; tetrahydrofuran, toluene, and n-hexane were dried by refluxing, under argon, with Na, degassed and distilled prior to use. Deuterated solvents, benzene-d_6 and toluene-d_8, were dried over Na and distilled. Acetone was dried on $CaSO_4$ and distilled from the same compound. Pyrazole was sublimed prior to use. Guaiacol was distilled under reduced pressure. $[UCl_2\{HB(pz)_3\}_2]$ (**1**) [15], $[UCl(OEt)\{HB(pz)_3\}_2]$ [18], $LiCH_2SiMe_3$ [19], $LiCH(SiMe_3)_2$ [20], $LiCH_2Ph$ [21], KCH_2Ph [22], $LiCH_2C_6H_4$-*o*-NMe_2 [23], LiC_6H_4-*o*-CH_2NMe_2 [24] were prepared as previously described. LiMe (1.6 M in diethylether) from Aldrich was used without further purification.

^{1}H NMR spectra were recorded on a Bruker SY80FT multinuclear spectrometer and referenced internally using the residual solvent resonance relative to tetramethylsilane. IR spectra were recorded as Nujol mulls on a Perkin–Elmer 577 spectrophotometer. Carbon, hydrogen and nitrogen analyses were performed on a Perkin–Elmer automatic analyser. [For some compounds we were unable to obtain accurate elemental analyses, especially for nitrogen, but the complexes could be unambiguously identified and their purity assessed by ^{1}H NMR spectroscopy.] Absorption electronic spectra were recorded as solutions on a Cary 2390 Varian spectrometer. The FTICR mass spectra were done, either by laser desorption (LD) or by electron impact (EI), with a 2001-DT instrument equipped with a 3.0 T superconducting magnet and interfaced to a Spectra-Physics Quanta-Ray GCR-11 pulsed Nd:YAG laser operating at the fundamental wavelength (1064 nm) with an estimated output of 20–50 mJ/pulse. Samples were prepared under argon in a glove box. Standard FTICR event sequences were employed, with the ions formed, trapped, excited and detected on the source side of the dual 'source/analyzer' ion trap.

2.2. Synthesis and characterization of $[UCl(Me)\{HB(pz)_3\}_2]$ (2)

Method 1. To a green suspension of **1** (250 mg, 0.34 mmol) in toluene was added dropwise MeLi (149 mg, 0.34 mmol) in toluene. After stirring for 2 h, at room temperature, a clear orange solution was obtained from which was recovered, after removal of the solvent, a salmon solid (122 mg, 0.17 mmol, 50% yield).

Method 2. To a solution of **5** (150 mg, 0.22 mmol) in 10 ml of toluene was added 160 mg (0.22 mmol) of **1**. The mixture was stirred during 7 days, centrifuged and the solution was taken to dryness in vacuo, yielding a salmon solid which was washed with n-hexane (203 mg, 0.28 mmol, 64% yield). Anal. Found: C, 31.96; H, 3.09; N, 22.50. $C_{19}H_{23}B_2N_{12}ClU$ Calc.: C, 31.94; H, 3.24; N, 23.52%. IR (Nujol, ν (cm^{-1})): 3100w, 2480m (ν(B–H)), 1490s, 1390s, 1370s, 1285s, 1250s, 1205s, 1180m, 1110s, 1080w, 1060m, 1040s, 965s, 910w, 790m, 770m, 750s, 710s, 650m, 610m, 460w, 340w. UV–vis (toluene) (λ_{max} (nm)): 1410m, 1250w, 1088s, 970w, 660s.

2.3. Synthesis and characterization of $[UCl(CH_2SiMe_3)\{HB(pz)_3\}_2]$ (3)

At room temperature, $LiCH_2SiMe_3$ (64 mg, 0.68 mmol) dissolved in toluene was added slowly to a suspension of **1** (500 mg, 0.68 mmol) in toluene. After stirring for 2 h the red suspension was centrifuged and the solution was taken to dryness in vacuo. The red solid was washed with n-hexane, and after drying, the solid obtained was formulated as **3** (372 mg, 0.47 mmol, 70% yield). Anal. Found: C, 34.11; H, 3.99; N, 20.62. $C_{22}H_{31}B_2N_{12}ClSiU$ Calc.: C, 33.59; H, 3.97; N, 21.36%. IR (Nujol, ν (cm^{-1})): 3100w, 2450m (ν(B–H)), 1500s, 1370s, 1290s, 1260m, 1230w, 1210s, 1190w, 1120m, 1060m, 1045s, 1020w, 970s, 920w, 885w, 850w, 800w, 780w, 790m, 750w, 720m, 670w, 610w. UV–vis (toluene) (λ_{max} (nm)): 1420m, 1270w, 1230w, 1150sh, 1110s, 1090s, 1065s, 960m, 800m.

2.4. Synthesis and characterization of [UCl(C_6H_4-o-CH_2NMe_2){$HB(pz)_3$}$_2$] (4)

This compound has been synthesized according to the procedure described above for **3**. Starting with 500 mg (0.68 mmol) of **1** and using 96 mg (0.68 mmol) LiC_6H_4-o-CH_2NMe_2 a yellow–brown solid was isolated and formulated as **4** (463 mg, 0.56 mmol, 82% yield). Anal. Found: C, 37.76; H, 3.83; N, 20.79. $C_{27}H_{32}B_2N_{13}ClU$ Calc.: C, 38.90; H, 3.89; N, 21.84%. IR (Nujol, ν (cm^{-1})): 3100w, 2470m (ν(B–H)), 1490m, 1390m, 1370s, 1290s, 1260m, 1210s, 1110s, 1040s, 970s, 915w, 840w, 800m, 750m, 720m, 660m, 610m. UV–vis (toluene) (λ_{max} (nm)): 1470m, 1190s, 1090s, 940w, 680m, 670s, 580w.

^1H NMR in toluene-d_8 at 220 K (δ (ppm)): 137.3 (1H), 75.5 (1H), 65.1 (1H, C_6H_4-o-CH_2NMe_2), 56.7 (1H, C_6H_4-o-CH_2NMe_2), 55.9 (1H), 55.2 (1H), 42.8 (1H, C_6H_4-o-CH_2NMe_2), 42.5 (1H, C_6H_4-o-CH_2NMe_2), 40.8 (1H), 35.2 (1H), 30.5 (1H, C_6H_4-o-CH_2NMe_2), 30.0 (1H), 23.9 (1H), 16.9 (1H), 15.9 (1 + 1H), 2.9 (1H, C_6H_4-o-CH_2NMe_2), −7.6 (1H, B–H), −8.0 (1H), −9.7 (3H, C_6H_4-o-CH_2NMe_2), −11.3 (1H), −13.8 (1H), −14.3 (1H), −15.5 (1H), −23.2 (1H), −26.9 (1H, B–H), −40.2 (3H, C_6H_4-o-CH_2NMe_2), −77.7 (1H).

2.5. Synthesis and characterization of [U(Me)$_2${$HB(pz)_3$}$_2$] (5)

At room temperature, a solution of MeLi (298 mg, 0.68 mmol) suspended in 25 ml of toluene, was slowly added to a slurry of **1** (250 mg, 0.34 mmol) in toluene. After work-up, as referred to for **3**, the yellow–brown solid obtained was formulated as **5** (158 mg, 0.23 mmol, yield 67%). Anal. Found: C, 34.61; H, 3.53; N, 23.18. $C_{20}H_{26}B_2N_{12}U$ Calc.: C, 34.62; H, 3.78; N, 24.22%. IR (Nujol, ν (cm^{-1})): 3100w, 2460m (ν(B–H)), 1390s, 1370s, 1290s, 1250m, 1205s, 1185m, 1065m, 1040s, 1005w, 970s, 910w, 790m, 770m, 760m, 750m, 740m, 710s, 660m, 640m, 570m, 460w sh, 400m, 340w, 325w. UV–vis (toluene) (λ_{max} (nm)): 1638w, 1407m, 1074s, 800w, 672w.

2.6. Synthesis and characterization of [U(CH_2SiMe_3)$_2${$HB(pz)_3$}$_2$] (6)

A solution of $LiCH_2SiMe_3$ (185 mg, 1.89 mmol) in 10 ml of toluene was added dropwise to a slurry of **1** (721 mg, 0.98 mmol) in the same solvent (10 ml). After work-up as indicated for **3**, 572 mg of a dark brown solid was obtained (0.68 mmol, 70% yield).

Anal. Found: C, 37.70; H 4.95; N, 19.56. $C_{26}H_{42}B_2N_{12}Si_2U$ Calc.: C, 37.24; H, 5.05; N, 20.04%. IR (Nujol mull, ν (cm^{-1})): 2450s (ν(B–H)), 1455w, 1430f, 1300s, 1260sh, 1250sh, 1240w, 1220s, 1195m, 1125s, 1065sh, 1050s, 975s, 865b, 760s, 725s, 670m, 620m, 350m. UV–vis (toluene) (λ_{max} (nm)): 1443sh, 1367s, 1120sh, 1090sh, 1076s, 932w, 683s.

2.7. Synthesis and characterization of [UCl(pz){$HB(pz)_3$}$_2$]) (7)

9 mg (0.13 mmol) of pzH was added to a stirred solution of [UCl(C_6H_4-o-CH_2NMe_2){$HB(pz)_3$}$_2$] (110 mg, 0.13 mmol) in toluene (5 ml) at room temperature. The colour of the solution instantaneously changed from brown–red to light green. The reaction was stirred for 1 h, after which the solvent was removed under reduced pressure to yield a bright green solid. The product was washed with minimal n-hexane and dried in vacuo. This compound was obtained in almost quantitative yield. IR (Nujol mull, ν (cm^{-1})): 2450m (ν(B–H)), 1500m, 1400s, 1380sh, 1300s, 1260m, 1215s, 1195sh, 1120s, 1061sh, 1050s, 980s, 920m, 800sh, 780sh, 760s, 720s, 620w, 600w, 590m, 335w, 260w. UV–vis (toluene) (λ_{max} (nm)): 1560(58) 1440(49), 1188sh, 1165(69), 1120sh, 1070(100), 670(118).

2.8. Synthesis and characterization of [U(pz)$_2${$HB(pz)_3$}$_2$] (8)

This compound was synthesized as referred to above for **7**. Starting with 16 mg (0.23 mmol) of pzH and 79 mg (0.11 mmol) of **5** in toluene (5 ml), **8** was obtained in almost quantitative yield. IR (Nujol mull, ν (cm^{-1})): 2450m (ν(B–H)), 1500m, 1400s, 1375m, 1360sh, 1350sh, 1300w, 1280sh, 1260f, 1210w, 1195sh, 1120w, 1065sh, 1050w, 1000w, 975s, 800w, 750s, 720s, 660m, 620s, 600w, 580m, 340w, 250w. UV–vis (toluene) (λ_{max} (nm)): 1560(113) 1380(84), 1170sh, 1190(157), 1000sh, 665(109).

^1H NMR in CD_2Cl_2 at 215 K (δ (ppm)): 42.1 (2H, *pz*), 35.5 (2H, *pz*), 34.6 (2H, H(4), *pz*), 32.8 (6H), 6.4 (6H), −2.9 (6H), −25.2 (2H, *B–H*).

2.9. Synthesis and characterization of [U(OC_6H_4-o-OMe)$_2${$HB(pz)_3$}$_2$] (9)

34 mg (0.27 mmol) of HOC_6H_4-o-OMe was added to a stirred solution of **6** (112 mg, 0.13 mmol) in toluene (5 ml) at room temperature. The colour of the solution changed from brown–red to bright green. The reaction was stirred for 1 h, after which the solvent was removed under reduced pressure to yield a bright green microcrystalline solid in almost quantitative yield (116 mg, 0.13 mmol). Anal. Found: C, 42.21; H, 4.02; N, 18.44. $C_{32}H_{34}B_2N_{12}O_4U$ Calc.: C, 42.22; H, 3.76; N, 18.46%. IR (Nujol mull, ν (cm^{-1})): 2440m (ν(B–H)), 1480m, 1400s, 1300w, 1290w, 1255m, 1215m, 1190w, 1120m, 1105sh, 1060w, 1045m, 1020w, 970m, 870w, 800w, 770sh, 760w, 730m, 715m, 660w, 610w, 600w, 490w. UV–vis (toluene) (λ_{max} (nm)): 1440w, 1328m, 1130sh, 1100s, 1066s, 667s.

2.10. Synthesis and characterization of $[U\{OCMe_2CH_2SiMe_3\}_2\{HB(pz)_3\}_2]$ (10)

Acetone (28 mg, 0.48 mmol) was added to a stirred solution of **6** (100 mg, 0.12 mmol) in toluene (5 ml). Upon addition, the colour of the solution turned from brown–red to green. After stirring for 10 min the solvent was stripped off under vacuum, and the residue was washed with hexane (5 ml). Compound **10** is obtained as a dark green microcrystalline solid (50 mg, 0.052 mmol, 44% yield). Anal. Found: C, 41.03; H, 4.74; N, 17.53. $C_{32}H_{54}B_2N_{12}O_2Si_2U$ Calc.: C, 40.26; H, 5.70; N, 17.61%. IR (Nujol mull, ν (cm^{-1})): 2475s (ν(B–H)), 1700m, 1495s, 1400s, 1375s, 1350vw, 1300s, 1260m, 1215s, 1195vw, 1155vw, 1120m, 1055m sh, 1050m, 970m, 800m, 780m, 760m, 720s, 660w, 620m. UV–vis (toluene) (λ_{max} (nm)): 1600s, 1235s, 976s, 572w.

^{1}H NMR in toluene-d_8 at 220 K (δ (ppm)): 65.9 (2H), 35.5 (2H), 21.7 (2H) 21.2 (2H, $\{OCMe_2CH_2SiMe_3\}$), 19.3 (6H, $\{OCMe_2CH_2SiMe_3\}$), 16.8 (6H, $\{OCMe_2CH_2SiMe_3\}$), 14.5 (2H, $\{OCMe_2CH_2SiMe_3\}$), 10.8 (2H), 7.5 (2H), 4.1 (18H $\{OCMe_2CH_2SiMe_3\}$), 1.9 (2H), −10.0 (2H), −10.9 (2H), −16.2 (2H, B–H), −20.4 (2H).

2.11. Synthesis and characterization of $[UCl\{OCMe_2CH_2(C=O)Me\}\{HB(pz)_3\}_2]$ (11)

Acetone (24 mg, 0.41 mmol) was added to a stirred solution of **4** (125 mg, 0.15 mmol) in toluene (5 ml). Upon addition the colour of the solution turned from brown–red to bright green. After stirring for 30 min the solvent was stripped off under vacuum, and the residue was washed with hexane (5 ml). Compound **11** is obtained as a bright green microcrystalline solid (121 mg, 0.14 mmol, 99% yield). Anal. Found: C, 33.90; H, 2.47; N, 20.92. $C_{24}H_{31}B_2N_{12}O_2ClU$ Calc.: C, 35.38; H, 3.84; N, 20.63%. IR (Nujol mull, ν (cm^{-1})): 2450s (ν(B–H)), 1705m (ν(C=O)), 1500s, 1400s, 1340s, 1300s, 1265m, 1220s, 1200sh, 1125s, 1065sh, 1055s, 975s, 955w, 925w, 810w, 785sh, 766sh, 725s, 700w, 670w, 625m, 340m, 245m. UV–vis (toluene) (λ_{max} (nm)): 1450s, 1385s, 1280s, 1140sh, 1080sh, 1035s, 970sh, 660sh, 640m, 620sh.

2.12. Synthesis and characterization of $[UCl\{OCMe_2CH_2SiMe_3\}\{HB(pz)_3\}_2]$ (12)

1 (303 mg, 0.41 mmol), acetone (24 mg, 0.41 mmol) and $LiCH_2SiMe_3$ (39 mg, 0.41 mmol) react in toluene providing, after work-up, a green solid which was formulated as **12** (239 mg, 68%). Anal. Found: C, 35.90; H, 3.80; N, 20.0. $C_{25}H_{37}B_2N_{12}OSiClU$ Calc.: C, 35.54; H, 4.41; N, 19.90%. IR (Nujol mull, ν (cm^{-1})): 2460m (ν(B–H)), 1500m, 1460s, 1400m, 1370s, 1290m, 1260m, 1215m, 1190w, 1120m, 1065w, 1050s, 1015sh w, 975m, 860w, 800w, 760m, 720m, 660w, 610w. UV–vis (toluene) (λ_{max} (nm)): 1400m, 1330m, 1145sh, 995s, 1066s, 660w.

Table 1
Crystallographic data for $[U(OC_6H_4\text{-}o\text{-}OMe)_2\{HB(pz)_3\}_2]$ (**9**) and $[UCl(Hpz)(O^tBu)((\mu\text{-}O)B(\mu\text{-}pz)(pz)_2)]_2$ (**13**)

Compound	**9**	**13**
Formula	$C_{32}H_{34}B_2N_{12}O_4U$	$C_{32}H_{44}B_2Cl_2N_{16}O_4U_2$
Mol. wt.	910.34	1285.42
Crystal system	Triclinic	Monoclinic
Space group	$P\bar{1}$	$P2_1/n$
a (Å)	12.295(2)	13.701(3)
b (Å)	12.640(2)	11.337(2)
c (Å)	13.994(2)	14.857(4)
α (deg)	76.10(1)	90
β (deg)	72.50(1)	104.65(2)
γ (deg)	80.71(1)	90
V (Å^3)	2004(2)	2233(1)
Z	2	2
ρ_{calc} (g cm^{-3})	1.509	1.912
Linear abs. coeff. (cm^{-1}) (Mo Kα)	39.00	74.18
2θ Range (deg)	3.0–54.0	3.0–52.0
Decay corr. factors: min., max.	1.00001, 1.03385	1.00020, 1.47871
Range in absorbance correction factors	0.8971, 0.9976	0.5459, 0.9996
Number of reflections	7686	3249
Number of parameters refined	406	266
Refinement method	F	F^2
R_1 [a]	0.038 ($F_o > 3\sigma(F_o)$)	0.0515 ($F_o > 4\sigma(F_o)$)
R_w [b]	0.043 ($F_o > 3\sigma(F_o)$)	0.1169 ($F_o > 4\sigma(F_o)$)

[a] $R_1 = \Sigma||F_o| - |F_c||/\Sigma|F_o|$.

[b] For **9** $R_w = [\Sigma w||F_o| - |F_c||^2/\Sigma w|F_o|^2]^{1/2}$, $w = [\sigma^2(F_o^2)]^{-1}$. For **13** $R_w = [\Sigma(w(F_o^2 - F_c^2)^2)/\Sigma(w(F_o^2)^2)]^{1/2}$; $w = 1/[\sigma^2(F_o^2) + (0.0817P)^2]$, where $P = (\max(F_o^2,o) + 2F_c^2)/3$.

2.13. X-ray crystallographic analysis of $[U(OC_6H_4\text{-}o\text{-}OMe)_2\{HB(pz)_3\}_2]$ (9)

A bright green crystal of approximate dimensions $0.54 \times 0.32 \times 0.29\,mm^3$, obtained by slow diffusion of n-hexane into a saturated solution of the compound in toluene, was mounted in a thin-walled glass capillary in an argon filled glove-box. Data were collected at room temperature on an Enraf–Nonius CAD-4 diffractometer with graphite-monochromated Mo Kα radiation, using an ω–2θ scan mode. Unit cell dimensions were obtained by least-squares refinement of the setting angles of 25 reflections with $17.2° < 2\theta < 31.9°$. Details of the crystal data, data collection and refinement are given in Table 1. Data were corrected for Lorentz–polarization effects, for linear decay (−6.4% in 133.3 h) and for absorption by empirical corrections based on ψ scans, using the Enraf–Nonius program. The structure was solved by Patterson methods [25] and subsequent difference Fourier techniques [26]. There is one molecule of crystallization solvent in the lattice (toluene or hexane), the disorder of which could not be modelled. It was taken into account considering the three strongest peaks in the residual electron density map as full-occupancy carbon atoms. As no chemical identity could be assigned to the lattice solvent, it was then excluded from the formula, from the molecular weight and from the calculation of the density in Table 1. All but the solvent and the carbon atoms of the phenoxide ligands were refined anisotropically. The hydrogen atoms were introduced in calculated positions (except those of the solvent) constrained to ride on their carbon and boron atoms with group U_{iso} values assigned. In the final difference-Fourier map the highest peak was $1.1\,e\,Å^{-3}$ and was near the U atom. Three strong reflections (−110, 101, 011) which were thought to be affected by extinction were omitted from the data. Final atomic coordinates are listed in Table 2. Atomic scattering factors and anomalous dispersion terms were taken from the International Tables for X-ray Crystallography.

2.14. X-ray crystallographic analysis of $[UCl(Hpz)(O^tBu)\{(\mu\text{-}O)B(\mu\text{-}pz)(pz)_2\}]_2$ (13)

A green crystal of approximate dimensions $0.31 \times 0.18 \times 0.16\,mm^3$, obtained during the recrystallization of a mixture of $[UCl(O^tBu)\{HB(pz)_3\}_2]$ and **11**, was mounted in a thin-walled glass capillary in an argon filled glove-box. Data were collected at room temperature, as described for **9**. Unit cell dimensions were obtained by least-squares refinement of the setting angles of 25 reflections with $15.49° < 2\theta < 29.76°$. Data were corrected [27] for Lorentz–polarization effects, for linear decay (−54.3% in 47.9 h) and for absorption (ψ scans). The structure was solved by Patterson methods [25] and refined on F^2 by full-matrix least-squares

Table 2
Fractional atomic coordinates ($\times 10^4$) and thermal parameters for $[U(OC_6H_4\text{-}o\text{-}OMe)_2\{HB(pz)_3\}_2]$ (9)

Atom	x	y	z	U_{eq} [a] / U_{iso} [b] ($\times 10^3 Å^2$)
U	2420.7(2)	2492.3(2)	2413.6(2)	33(1)
O(1)	2356(4)	2302(4)	3979(3)	54(2)
O(2)	4220(4)	2178(4)	2061(4)	54(2)
O(3)	970(5)	3338(5)	5411(4)	85(3)
O(4)	5634(5)	1173(5)	616(5)	85((3)
N(1)	2860(5)	400(4)	2624(4)	53(2)
N(2)	588(5)	1580(5)	3459(4)	53(2)
N(3)	1698(5)	1761(4)	1111(4)	50(2)
N(4)	712(4)	3864(4)	1994(4)	51(2)
N(5)	3200(5)	3704(5)	630(4)	57(2)
N(6)	2612(5)	4389(4)	2649(4)	53(2)
N(11)	2099(5)	−302(4)	2670(4)	57(3)
N(21)	207(5)	722(5)	3265(4)	59(3)
N(31)	1133(5)	848(5)	1382(4)	53(2)
N(41)	849(5)	4901(5)	1431(5)	58(2)
N(51)	2872(5)	4788(5)	341(4)	61(2)
N(61)	2442(6)	5356(5)	1996(5)	62(3)
C(1) [b]	2466(5)	1999(5)	4938(5)	49(2)
C(2) [b]	3285(7)	1170(6)	5157(6)	66(2)
C(3) [b]	3383(9)	833(9)	6171(8)	93(3)
C(4) [b]	2678(9)	1375(9)	6891(8)	96(3)
C(5) [b]	1863(8)	2206(8)	6701(8)	86(3)
C(6) [b]	1748(7)	2525(6)	5702(6)	62(2)
C(30) [b]	228(12)	3895(11)	6170(10)	138(5)
C(14) [b]	5344(5)	2040(5)	1986(5)	46(1)
C(15) [b]	5753(6)	2369(6)	2670(5)	57(2)
C(16) [b]	6930(7)	2220(7)	2602(7)	76(2)
C(17) [b]	7663(8)	1736(8)	1848(7)	82(2)
C(18) [b]	7275(7)	1370(7)	1171(6)	71(2)
C(19) [b]	6111(6)	1512(6)	1239(5)	56(2)
C(40) [b]	6356(10)	602(9)	−111(9)	107(3)
C(7) [b]	5484(20)	3995(17)	4818(17)	194(8)
C(8) [b]	4524(19)	4174(16)	5458(15)	178(7)
C(9) [b]	3672(19)	5088(21)	5862(17)	218(9)
C(11)	2569(9)	−1335(6)	2887(7)	79(4)
C(12)	3640(9)	−1312(6)	2994(7)	80(4)
C(13)	3783(7)	−214(6)	2821(6)	64(3)
C(21)	−817(7)	521(8)	3927(7)	77(3)
C(22)	−1120(7)	1253(9)	4567(6)	86(4)
C(23)	−214(6)	1891(7)	4255(5)	68(3)
C(31)	704(7)	756(7)	633(6)	67(4)
C(32)	1007(7)	1619(7)	−164(6)	71(4)
C(33)	1614(6)	2225(6)	170(5)	61(3)
C(41)	−136(8)	5349(8)	1207(7)	81(4)
C(42)	−919(7)	4609(9)	1604(7)	86(5)
C(43)	−367(6)	3683(7)	2090(6)	66(3)
C(51)	3540(9)	5166(10)	−606(7)	93(5)
C(52)	4285(8)	4339(11)	−948(7)	106(5)
C(53)	4070(7)	3433(8)	−151(6)	81(4)
C(61)	2761(8)	6165(7)	2283(7)	81(5)
C(62)	3125(8)	5737(6)	3156(7)	76(4)
C(63)	3026(6)	4623(6)	3348(6)	59(3)
B(1)	935(8)	90(7)	2456(7)	60(4)
B(2)	1983(9)	5416(7)	1084(8)	69(4)

[a] U_{eq} is defined as one-third of the trace of the orthogonalized U_{ij} tensor.
[b] Isotropic temperature factors were used.

Table 3
Fractional atomic coordinates ($\times 10^4$) and thermal parameters for $[UCl(Hpz)(O^tBu)\{(\mu\text{-}O)B(\mu\text{-}pz)(pz)_2\}]_2$

Atom	x	y	z	U_{eq} ($\times 10^3$ Å^2)
U(1)	3813.6(4)	475.9(3)	433(3)	29(1)
Cl(1)	2506(3)	−221(3)	−1198(2)	48(1)
O(1)	5113(7)	−900(7)	480(6)	37(2)
O(2)	2674(8)	1030(8)	993(7)	44(2)
N(1)	3284(8)	−1749(9)	638(9)	40(3)
N(2)	4721(9)	−295(9)	2093(8)	44(3)
N(3)	6578(9)	−2430(8)	501(8)	41(3)
N(4)	4930(9)	2095(8)	1401(8)	39(3)
N(11)	4138(9)	−2472(8)	854(8)	38(3)
N(21)	5265(8)	−1290(8)	2097(7)	34(2)
N(31)	6022(10)	−2681(9)	1094(8)	43(3)
N(41)	5921(10)	2116(10)	1678(8)	48(3)
C(2)	1796(11)	1214(13)	1355(13)	52(4)
C(11)	3766(16)	−3597(12)	760(11)	68(6)
C(12)	2770(16)	−3604(14)	507(13)	75(6)
C(13)	2506(13)	−2418(12)	445(13)	65(5)
C(21)	5716(12)	−1603(13)	2981(11)	49(4)
C(22)	5454(14)	−764(15)	3545(12)	63(5)
C(23)	4821(13)	13(14)	2970(11)	53(4)
C(31)	6351(13)	−3695(12)	1552(11)	57(4)
C(32)	7132(13)	−4119(12)	1236(11)	55(4)
C(33)	7255(13)	−3306(12)	577(11)	54(4)
C(41)	6260(13)	2967(12)	2296(12)	58(5)
C(42)	5436(12)	3559(12)	2423(13)	60(5)
C(43)	4624(14)	2996(12)	1848(13)	60(5)
C(211)	1667(19)	189(17)	1892(19)	104(9)
C(212)	910(17)	1313(20)	554(19)	115(9)
C(213)	1945(16)	2329(15)	1908(16)	81(6)
B(1)	5152(12)	−1841(12)	1110(12)	38(4)

techniques [28]. All non-hydrogen atoms were refined anisotropically and the hydrogen atoms were introduced in idealized positions. A final difference-Fourier synthesis revealed some residual electron density around the uranium, between −3.68 and +1.05 e Å^{-3}, probably due to the great decay of the crystal measured and consequently inefficient absorption correction. Crystallographic data and coordinates of the non-hydrogen atoms are given in Tables 1 and 3. Atomic scattering factors and anomalous dispersion terms were as in SHELXL-93.

3. Results and discussion

3.1. Synthesis of chlorohydrocarbyl and bis(hydrocarbyl) complexes

In toluene and at room temperature the dichloride $[UCl_2\{HB(pz)_3\}_2]$ (**1**) can be alkylated with some alkyl and aryl lithium reagents according to Scheme 1.

These crystalline compounds, extremely air and moisture sensitive, can be obtained in reasonable yields (60–80%). They were characterized by IR and ^{1}H NMR spectroscopy, by elemental analysis and in the case of **4** by FTICR/MS. The FTICR/MS was tried for all the hydrocarbyls, as well as for the mixed alkoxide–hydrocarbyl derivatives. For **4** the mass spectra were clear and confirmed unambiguously the presence of the complex, for the others the molecular ions could never be observed, not even ionic fragments containing the hydrocarbyl moieties, due to the thermal instability of the compounds. **4**: LD (−): 833 (100%), M$^-$; EI (−) [180 °C/ − 70 eV]: 833 (100%), M$^-$; 213 (25%) $\{HB(pz)_3\}^-$.] The colour of the complexes depends on the nature and on the number of the alkyl groups coordinated to the uranium, being salmon, yellow–brown, dark brown or red. The bis(hydrocarbyl) derivatives are soluble in aromatic and aliphatic hydrocarbon solvents and the chlorohydrocarbyls are soluble in aromatic but only slightly soluble in aliphatic solvents.

Reactions of $[UCl_2\{HB(pz)_3\}_2]$ (**1**) with MCH_2Ph (M = Li, K), $LiCH_2C_6H_4$-*o*-NMe_2, $LiCH_2CMe_3$ or with $LiCH(SiMe_3)_2$ in different stoichiometries and in different solvents (toluene, tetrahydrofuran or ether) have been tried but no uranium(IV) hydrocarbyls could be isolated. In these reactions, either we obtained unidentified products ($LiCH_2CMe_3$) or we observed the formation of a bright green product, very soluble in toluene, with an absorption electronic spectrum characteristic of U(III) [29,30] (in toluene; λ_{max} (nm): 740sh, 930s, 980sh, 995m, 1010sh, 1070w, 1085w, 1100sh, 1185sh, 1230s, 1240sh, 1545m), and with an IR spectrum indicating the presence of the hydro(trispyrazolyl)borate ligand, namely the ν(B–H) stretching band at 2464 cm^{-1} (ν(B–H) in the K salt of the ligand: 2420 cm^{-1}, ν(B–H) in **1**: 2480 cm^{-1}) [15]. The ^{1}H NMR spectrum of this species in toluene-d_8 or in benzene-d_6 presented three broad resonances of equal intensity at 15.5, 7.5 and −0.2 ppm. Variable temperature ^{1}H NMR studies indicate that no dynamic process was involved and the broad resonances observed in this species were probably related with the oxidation state of the metal centre [31]. This U(III) species reacts very quickly with ethanol and with dichloromethane or chloroform leading to the known compounds $[UCl(OEt)\{HB(pz)_3\}_2]$ [18] and $[UCl_2\{HB(pz)_3\}_2]$ (**1**) [15] respectively. Analogous reduced species was also obtained by reacting **1** with Li^{t}Bu [32] which is a well known method to prepare U(III) compounds from U(IV) chlorocomplexes [33]. All the attempts that have been made to obtain crystals of this U(III) species did not succeed, and we always observed its decomposition during recrystallization with formation of a brown product. This product was insoluble in aromatic, aliphatic and chlorinated solvents, so it was only analysed by infrared spectroscopy, elemental analysis and by FTICR-MS. {IR (Nujol mull, ν (cm^{-1})): 2449 (B–H), 1508, 1409, 1381, 1304, 1297, 1213, 1125, 1050, 977, 773, 756, 727, 675, 629. FTICR/MS: (m/z referenced

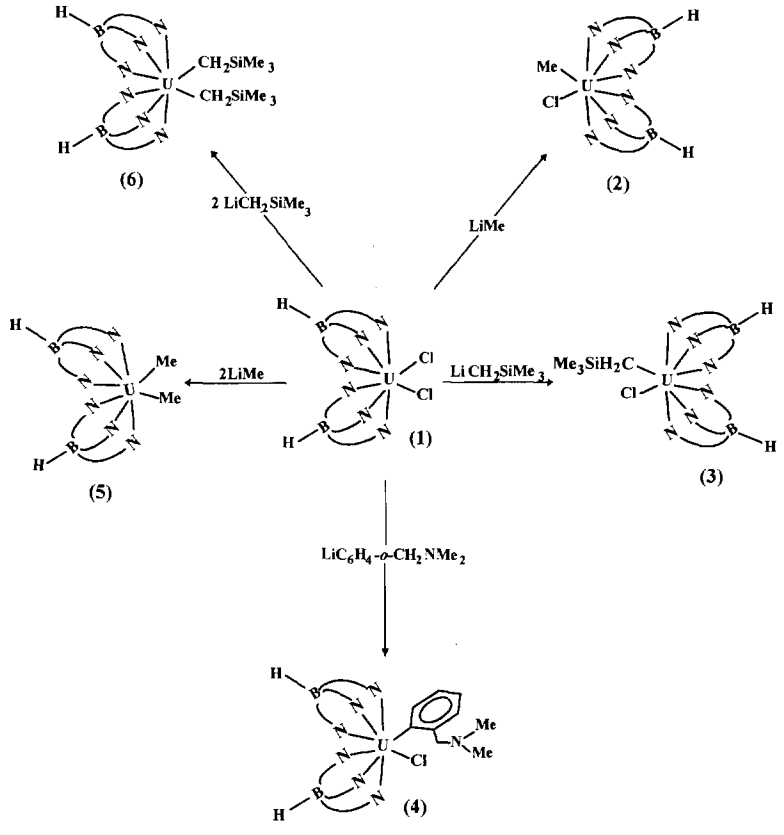

Scheme 1. Syntheses of σ-hydrocarbyl derivatives of $[UCl_2\{HB(pz)_3\}_2]$ (**1**).

to the species with ^{11}B; relative abundance in parentheses) LD(+): 731 (25%) $[U(pz)\{HB(pz)_3\}_2]$; 664 (100%) $[U\{HB(pz)_3\}_2]$; 585 (25%) $[U(pz)_2\{HB(pz)_3\}]$. Elemental analysis for $[U(pz)\{HB(pz)_3\}_2]_x$ Anal. Found: U, 33.10; C, 35.06; H, 3.39; N, 26.59. $C_{21}H_{23}B_2N_{14}$ Calc.: U, 32.56; C, 34.51; H, 3.15; N, 26.84%.} From the results obtained we could only confirm the presence of $\{HB(pz)_3\}$ coordinated to the uranium and the absence of halogen. This result seems to indicate that during recrystallization, probably due to a redistribution process, the chloride was replaced either by another ligand or by pyrazole resulting from decomposition. Redistribution reactions have frequently been observed in the chemistry of Ln(III) complexes with poly(pyrazolyl)borate ligands [34].

Using the analogous $[UCl_2(C_5Me_5)_2]$, Marks and coworkers [11] isolated a large variety of chloro and bis(hydrocarbyls), including the benzyl and neopentyl derivatives, which has been impossible using the precursor $[UCl_2\{HB(pz)_3\}_2]$. However the stability of the hydrocarbyls described in this work seems to compare with the variation in the metal–alkyl bond disruption enthalpies determined for compounds $[AnRCl(C_5Me_5)_2]$ and $[AnR_2(C_5Me_5)_2]$ (An = U, Th), which indicates D(U–R) for $CH_3 \geq CH_2SiMe_3 > CH_2Ph \approx CH_2CMe_3$ [35–37]. If we assume that the benzyl derivative with the unit '$[U\{HB(pz)_3\}_2]$' is not stable due to stereochemical factors, it is difficult to explain the stability of **2**, and the use of more bulky ligands, such as $LiCH_2C_6H_4$-o-NMe_2 or $LiCH(SiMe_3)_2$, would satisfy the unsaturation leading to compounds with stable U–C bonds. Reduction of U(IV) → U(III) by lithium alkyls has already been observed by others, although there is some controversy concerning the mechanism of the reduction process [7,38]. In our case the lithium salt cannot be responsible for the reduction observed, as we obtained an analogous result even using KCH_2Ph to prepare the benzyl derivative. Also interesting was the stabilization of the mixed $[U(CH_2Ph)(OEt)\{HB(pz)_3\}_2]$, obtained by reacting $[UCl(OEt)\{HB(pz)_3\}_2]$ with $LiCH_2C_6H_5$ in toluene (^1H NMR data in Table 4) [16]. The high electropositive character of the uranium metal is certainly modulated by supporting ligands, and this modulation is related with their electron donor character. The X-ray crystallographic analysis for $[UCl(OEt)\{HB(pz)_3\}_2]$ [18] indicated a very short U–O bond and an almost linear U–O–C bond angle, which in some complexes of uranium has been considered as evidence of strong π-bonding between the U and the O atoms [9]. This assumption and a weaker electron donor character of the $\{HB(pz)_3\}^-$ compared to $(C_5Me_5)^-$ may explain the disruption of the uranium–carbon bond in the benzyl derivatives, with the consequent reduction of the metal, and the stabilization of $[U(CH_2Ph)(OEt)\{HB(pz)_3\}_2]$.

As referred to previously by Marks and coworkers

Table 4
^{1}H NMR data for hydrocarbyls at room temperature [a]

Complex	{HB(pz)$_3$}				Other resonances
	H(3)	H(4)	H(5)	(B–H)	
[UCl(Me){HB(pz)$_3$}$_2$] (**2**)	29.7 (6H)	6.7 (6H)	−0.4 (6H)	−17.4 (2H)	205.7 (3H, 1w = 20 Hz, Me)
[UCl(CH$_2$SiMe$_3$){HB(pz)$_3$}$_2$] (**3**)	24.1 (6H)	6.6 (6H)	0.9 (6H)	−15.2 (2H)	242.4 (2H, 1w = 19 Hz, CH$_2$) 26.0 (9H, 1w = 16 Hz, Me)
[UCl(C$_6$H$_4$-*o*-CH$_2$NMe$_2$){HB(pz)$_3$}$_2$] (**4**)	(6H)	(6H)	−5.6 (6H)	(2H)	30.8 (2H, 1w = 15 Hz, CH$_2$) −15.9 (6H, 1w = 15 Hz, Me)
[U(Me)$_2${HB(pz)$_3$}$_2$] (**5**)	29.5 (6H)	6.6 (6H)	−0.5 (6H)	−17.1 (2H)	42.6 (6H, 1w = 20 Hz, Me)
[U(CH$_2$SiMe$_3$)$_2${HB(pz)$_3$}$_2$] (**6**)	24.3 (6H)	6.8 (6H)	1.4 (6H)	−13.2 (2H)	55.2 (4H, 1w = 19 Hz, CH$_2$) 4.6 (18H, 1w = 16 Hz, Me)
[U(Me)(OEt){HB(pz)$_3$}$_2$]	29.9 (6H)	6.6 (6H)	−0.2 (6H)	−16.7 (2H)	147.9 (2H, 1w = 20 Hz, CH$_2$) 56.9 (3H, 1w = 20 Hz, Me) −133.3 (3H, 1w = 20 Hz, Me)
[U(CH$_2$SiMe$_3$)(OEt){HB(pz)$_3$}$_2$]	31.9 (6H)	7.1 (6H)	0.3 (6H)	−16.0 (2H)	142.0 (2H, 1w = 19 Hz, CH$_2$) 53.6 (3H, 1w = 16 Hz, Me) −126.2 (2H, 1w = 19 Hz, CH$_2$) −11.8 (9H, 1w = 16 Hz, Me)
[U(CH$_2$Ph)(OEt){HB(pz)$_3$}$_2$]	32.7 (6H)	7.0 (6H)	0.0 (6H)	−16.9 (2H)	162.0 (2H, 1w = 19 Hz, CH$_2$) 61.13 (3H, 1w = 16 Hz, Me) −155.9 (2H, 1w = 19 Hz, CH$_2$) −10.0 (2H, 1w = 16 Hz, *o*-H) 5.9 (2H, 1w = 16 Hz, *m*-H) 7.7 (1H, 1w = 16 Hz, *p*-H)

[a] The chemical shifts are in ppm from TMS; downfield shifts are positive; all the spectra were run in toluene-d_8.

[11], redistribution between dialkyl and dichloride complexes can be an alternative route to prepare chloro alkyl derivatives, and with the compounds [UCl$_2$(C$_5$Me$_5$)$_2$] and [UR$_2$(C$_5$Me$_5$)$_2$] (R = CH$_3$ and CH$_2$SiMe$_3$) it was found that the rate of redistribution was considerably faster for R = CH$_3$ than for R = CH$_2$SiMe$_3$. With the stabilizing ligands hydro(trispyrazolyl)borate this alternative route was also tried to prepare compounds **2** and **3**. Although with a slow rate, the reaction between **1** and **5** proceeds and **2** can be isolated in 60% yield (Eq. (2)). However, between **1** and **6** no redistribution is observed. These results indicate that the intermolecular alkyl transfer is more difficult in the system [UX$_2${HB(pz)$_3$}$_2$] (X = Cl, R) than with the cyclopentadienyl derivatives. In this case the steric bulk of the {HB(pz)$_3$}$^-$ (2.90) compared to (C$_5$Me$_5$)$^-$ (2.49) may play a determining role [39].

$$\underset{\mathbf{1}}{[UCl_2\{HB(pz)_3\}_2]} + \underset{\mathbf{5}}{[U(Me)_2\{HB(pz)_3\}_2]} \xrightarrow[\text{r.t., 7 days}]{\text{toluene}} 2\underset{\mathbf{2}}{[UCl(Me)\{HB(pz)_3\}_2]} \quad (2)$$

3.2. Reactions with protic substrates

In an exploratory study we evaluated the reactivity of **2–6** with pyrazole and with several alcohols, namely ethanol, isopropanol, tert-butanol and guaiacol. **2**, **3** and **4** react with pyrazole and with alcohols in 1:1 molar ratio leading to [UCl(pz){HB(pz)$_3$}$_2$] (**7**) and [UCl(OR){HB(pz)$_3$}$_2$] respectively. When the same compounds react with excess of pyrazole or alcohols, only **7** is formed in the reaction with pyrazole, but a mixture of species [UCl(OR){HB(pz)$_3$}$_2$] and [U(OR)$_2${HB(pz)$_3$}$_2$] is obtained in the reactions with alcohols. This is not unexpected, as we observed that [UCl$_2${HB(pz)$_3$}$_2$] reacts with ROH but not with Hpz.

5 and **6** react in the 1:2 molar ratio with the same substrates leading to [U(pz)$_2${HB(pz)$_3$}$_2$] (**8**) or [U(OR)$_2${HB(pz)$_3$}$_2$] respectively. When **5** or **6** react with alcohols in 1:1 molar ratio the ^{1}H NMR spectrum of the crude reaction shows resonances due to unreacted bisalkyl (**5** or **6**) in addition to the species [U(OR)$_2${HB(pz)$_3$}$_2$], which is an indication that this is not a convenient process to prepare species of the type [UR(OR){HB(pz)$_3$}$_2$]. Protolysis of actinide-to-carbon σ bonds by alcohols is a process which has precedent in the literature, namely with the analogous [UMe$_2$(C$_5$Me$_5$)$_2$] [11]. However, for this system it was possible to detect the intermediate alkoxy alkyl compound when bulky alcohols, such as tert-butyl, were used. Cleavage of the uranium-hydro(trispyrazolyl)borate bonds was not observed, which is a difference relative to compounds with cyclopentadienyls, that in certain conditions are not spectator ligands [11,40]. Bispentamethylcyclopentadienyl pyrazolate derivatives, [U(pz)$_2$(C$_5$Me$_5$)$_2$] and [UCl(pz)(C$_5$Me$_5$)$_2$], have also been synthesized, although prepared by a different method [41].

The driving force for these reactions is undoubtedly the formation of strong U–O and U–N bonds. Thermochemical studies realized for uranium compounds containing a poly(pyrazolyl)borate ligand indicated that the cleavage of U–C bonds by alcohols was very exothermic, and the bond disruption energies found were, as expected, in the order D(U–O) > D(U–Cl) > D(U–N) > D(U-σ-C) [42]. The mechanism that has been suggested for these reactions involves coordination of the oxygen or nitrogen lone pair to the metal, followed by a four centre elimination of the alkane.

Some of the compounds formed by protolysis were characterized only by ^{1}H NMR by comparying the spectra obtained with the spectra of samples obtained on a preparative scale [43,44]. However, the new compounds **7** (Eq. (3)), **8** (Eq. (4)) and **9** (Eq. (5)) were isolated and characterized by the conventional methods, including X-ray crystallography for **9** (Section 2 and vide infra).

$$\underset{\mathbf{4}}{\left[UCl(C_6H_4\text{-}o\text{-}CH_2NMe_2)\{HB(pz)_3\}_2\right]} + Hpz \xrightarrow[\text{r.t.}]{\text{toluene}} \underset{\mathbf{7}}{\left[UCl(pz)\left\{HB(pz)_3\right\}_2\right]} + C_6H_5\text{-}o\text{-}CH_2NMe_2 \quad (3)$$

$$\underset{\mathbf{5}}{\left[U(Me)_2\left\{HB(pz)_3\right\}_2\right]} + 2Hpz \xrightarrow[\text{r.t.}]{\text{toluene}} \underset{\mathbf{8}}{\left[U(pz)_2\left\{HB(pz)_3\right\}_2\right]} + 2CH_4 \quad (4)$$

$$\underset{\mathbf{5}}{\left[U(Me)_2\left\{HB(pz)_3\right\}_2\right]} + 2HOC_6H_4\text{-}o\text{-}OMe \xrightarrow[\text{r.t.}]{\text{toluene}} \underset{\mathbf{9}}{\left[U(OC_6H_4\text{-}o\text{-}OMe)_2\{HB(pz)_3\}_2\right]} + 2CH_4 \quad (5)$$

7, **8** and **9** are green complexes all soluble in chlorinated solvents and **9** is also very soluble in aromatic and aliphatic solvents.

3.3. Reactions with acetone

Compounds **2** and **5** react with stoichiometric amounts of acetone yielding the alkoxides [UCl(O^{t}Bu)-{HB(pz)$_3$}$_2$] [44] and [U(O^{t}Bu)$_2${HB(pz)$_3$}$_2$] [44], due to the insertion of the acetone into the metal carbon bonds. These very fast reactions were studied by ^{1}H NMR spectroscopy, and the alkoxides were characterized by comparison with the ^{1}H NMR of samples obtained on a preparative scale [44]. The same type of insertion is observed when acetone reacts with **6**, but it has to be used in excess and the alkoxide [U(OCMe$_2$CH$_2$-SiMe$_3$)$_2${HB(pz)$_3$}$_2$] (**10**) is obtained in a relatively low yield (44%).

When the chlorohydrocarbyls **2**, **3** and **4** react with excess acetone we observed quantitative liberation of the respective alkane and the formation of one green complex that we suggest to be the aldolate derivative [UCl(OC(Me)$_2$CH$_2$C(=O)Me){HB(pz)$_3$}$_2$] (**11**), based on the IR and ^{1}H NMR. Further evidence for the formation of **11** was obtained as this compound gives the same IR and ^{1}H NMR spectra as those obtained by reacting **4** with 4-hydroxy-4-methyl-2-pentanone.

Compound **3** does not react with stoichiometric amount of acetone and using the molar ratio 1:2 we always obtained a mixture of **11** with another uranium(IV) species that we concluded to be the product of the insertion of acetone, [UCl(OCMe$_2$CH$_2$SiMe$_3$){HB(pz)$_3$}$_2$] (**12**). The characterization of **12** was made by comparison with the ^{1}H NMR of a sample obtained on a preparative scale, in one step synthesis by reacting **1** with Me$_2$CO and LiCH$_2$SiMe$_3$.

$$\underset{\mathbf{1}}{\left[UCl_2\left\{HB(pz)_3\right\}_2\right]} + Me_2CO + LiCH_2SiMe_3 \xrightarrow[\text{r.t., 1 h}]{\text{toluene}} \underset{\mathbf{12}}{\left[UCl(OCMe_2CH_2SiMe_3)\{HB(pz)_3\}_2\right]} + LiCl \quad (6)$$

10, **11** and **12** were characterized by IR, elemental analysis and ^{1}H NMR spectroscopy. A single crystal of **12**, obtained by recrystallization of a mixture of **11** and **12** from toluene/hexane, was measured. Although diffracting too weakly to provide sufficient data for satisfactory refinement of the structure, it was possible to establish the connections of the atoms in the molecule. [compound [UCl(OC(Me$_2$)CH$_2$SiMe$_3$){HB(pz)$_3$}$_2$] (**12**) crystallizes in the monoclinic space group $P2_1/a$ with cell parameters a = 15.778(2) Å, b = 25.922(5) Å, c = 17.038(3) Å, β = 101.21(3)°, V = 6836(3) Å^3; Z = 8.]

Insertion of ketones into metal–carbon σ bonds, with formation of metal alkoxides, is a common process for d- and f-transition elements, with several precedents in the literature [11,45]. Aldol condensation of ketones is not so common and, to the best of our knowledge, for f-elements it has been observed only for a reduced number of complexes: [(C$_5$Me$_5$)$_2$Th(Cl)–Ru(C$_5$Me$_5$)(CO)$_2$] [46], [Ln{CH(SiMe$_3$)$_2$}(C$_5$Me$_5$)$_2$] [47] and [UCl$_2${CH$_2$(SiMe$_3$)}{HB(3,5-Me$_2$pz)$_3$}] [48]. To explain the result Teuben and coworkers [47] considered the formation of an enolate intermediate by α-CH bond activation and coordination of a second molecule of acetone followed by C–C coupling. By contrast, Marks and coworkers [46] considered CH bond activation of the substrate, formation of a σ-hydrocarbyl and insertion of a second molecule of acetone into the metal carbon bond. In our case the reactions are very fast and no intermediates could be detected, it being difficult to discriminate between the two hypotheses which have been proposed [46,47]. However, all the chemistry that we have been doing with compounds containing the moiety '[U{HB(pz)$_3$}$_2$]' seems to indicate higher stability for M–O than for M–C bonds. Reactions of ketones with the U(III) {UCl$_2${HB(3,5-Me$_2$pz)$_3$}$_x$} lead also to

aldolate derivatives, which seems to indicate that the high Lewis acidity of the uranium centre is important in this type of reaction [48].

As referred to above, **2** reacts with acetone yielding either $[UCl(O^tBu)\{HB(pz)_3\}_2]$ or **11**. However, a mixture of both can also be obtained depending on the stoichiometry of the reagents. During the recrystallization of such a mixture, some crystals suitable for X-ray crystallographic analysis were obtained, and identified as $[UCl(Hpz)(O^tBu)\{(\mu\text{-}O)B(\mu\text{-}pz)(pz)_2\}]_2$ (**13**). Compound **13** is a dimer with modified poly(pyrazolyl)borate ligands (vide infra). The reduced amount of the green crystals obtained as well as their insolubility in toluene, benzene and chloroform, prevented us from performing any other analysis.

Although being generally assumed that poly(pyrazolyl)borate ligands represent an inert group, several examples are known in which these ligands themselves undergo reactions. These reactions may involve different degrees of ligand degradation, such as: deboronation, displacement of one pyrazole ring, attack of the hydrogen atom bound to the boron by electron rich groups, and boratropic rearrangements for the ligands with bulky groups in the pyrazole rings [29,30,49].

It is difficult to establish the mechanism responsible for the formation of **13**, as this was the only compound identified in a reaction where certainly other species are formed. However, no other uranium containing compounds were found in the supernatant solution, which can indicate that the moiety 'U–ClO^{t}Bu' is more stable than 'U–Cl{OC(Me)$_2$CH$_2$C(=O)Me}'. Assuming this, we may consider that the aldolate is released into the solution, due to decomposition of **11**, and may promote, as referred to by MacCleverty and coworkers [49], by an intermolecular process the deboronation of one $\{HB(pz)_3\}$ coordinated to the moiety 'U–ClO^{t}Bu'. Whether the attack of the B–H bond of the $\{HB(pz)_3\}$ which remains coordinated to the U is performed during the same process or by some residual humidity during recrystallization is not certain. The unsaturation of the coordination sphere of the uranium, when only one poly(pyrazolyl)borate is coordinate, is certainly responsible for the dimerization and for the coordination of an additional pzH, which exists in solution due to ligand deboronation.

3.4. IR spectra

All the uranium(IV) compounds present in the IR bands characteristic of the poly(pyrazolyl)borate ligands, namely the ν(B–H) stretching band that appeared between 2440 and 2480 cm^{-1}. The complexity of the spectrum of the $\{HB(pz)_3\}$ ligands does not allow us to identify unambiguously any band due to metal carbon, metal oxygen or metal nitrogen bonds. However, in the IR of **11** a strong absorption band at 1705 cm^{-1} could be clearly observed, which was assigned to ν(C=O). This band is shifted by 7 cm^{-1} relative to the corresponding stretching band in the free acetone, which appears at 1712 cm^{-1}. The relatively small shift to low energies is certainly an indication that this group is not coordinated to the uranium centre. So far, all the compounds isolated with the moiety 'U$\{HB(pz)_3\}_2$' are always eight-coordinate. Solid state structures as well as variable temperature ^{1}H NMR studies indicate that there is a large steric crowding around the uranium centre, with no additional position available for coordination of the C=O. The less sterically saturated compound $[UCl_2\{CH_2(SiMe_3)\}\{HB(3,5\text{-}Me_2pz)_3\}]$ reacts also with ketones leading to aldolate derivatives [48]. In this case a much larger shift to low energy was observed in the ν(C=O) relative to the free acetone ($\Delta\nu = 52$ cm^{-1}), and this was considered to be due to the coordination of the C=O group to the uranium. The complexes containing the moiety 'U$\{HB(3,5\text{-}Me_2pz)_3\}$' can be stabilized with coordination numbers of six or seven, depending on the steric bulk of the co-ligands [50], so such a coordination was not unexpected. This bidentate coordination of the aldolate was later confirmed by thermochemical studies, which indicate a uranium–oxygen bond dissociation enthalpy 20 kJ mol^{-1} higher than the D(U–O) values observed for alkoxide derivatives [51]. For the complex $[Ce\{OC(Me)_2CH_2C(=O)Me\}(C_5Me_5)_2]$ [47] the bidentate coordination of the aldol was confirmed by X-ray structural analysis and a decrease of 60 cm^{-1} in the ν(C=O) was also observed.

3.5. ^{1}H NMR spectra

In Tables 4 and 5 are presented the ^{1}H NMR data for **2–12** as well as for the mixed alkoxy–alkyl derivatives, which were only analysed by NMR spectroscopy.

Compounds **2**, **3**, **5**, **6**, **7–9**, **11** and **12** present only one set of resonances for the protons of the pyrazolyl rings, and one multiplet for the B–H protons. This is the pattern normally found in uranium complexes containing the moiety '$[U\{HB(pz)_3\}_2]$', in which the bulkiness of the co-ligands is not enough to slow down the dynamic process responsible for their fluxional behaviour in solution [50]. The chemical shifts of the resonances due to the H(3), H(4), H(5) and B–H protons are comparable to the chemical shifts of the corresponding protons in other compounds previously described with U–O, U–N and U–S bonds [43,52]. The resonances of the co-ligands all appear at low field, and for the chlorohydrocarbyls or chloroalkoxides they are shifted to lower field than the corresponding resonances in the bis(hydrocarbyl) or bis(alkoxide) derivatives. From the data presented in Table 4, an interesting feature is the dramatic change in the chemical shifts suffered by the protons of the alkyl groups when a chloride ligand is replaced by an alkoxide. [The prepara-

Table 5
^{1}H NMR data at room temperature [a]

Complex	{HB(pz)$_3$}				Other resonances
	H(3)	H(4)	H(5)	(B–H)	
[UCl(pz){HB(pz)$_3$}$_2$] (**7**)	20.1	6.8	3.3	−8.7	57.9 (2H, H(3), H(5))
	(6H)	(6H)	(6H)	(2H)	48.7 (1H, H(4))
[U(pz)$_2${HB(pz)$_3$}$_2$] (**8**)	22.7	6.1	0.7	−15.4	29.4 (4H, H(3), H(5))
	(6H)	(6H)	(6H)	(2H)	26.8 (2H, H(4))
[U(OC$_6$H$_4$-*o*-OMe)$_2${HB(pz)$_3$}$_2$] (**9**)	27.7	6.4	−0.2	−14.6	1.9 (6H, Me)
					24.2 (2H, d, J = 8 Hz, *o*-H)
	(6H)	(6H)	(6H)	(2H)	14.2 (2H, t, J = 8 Hz, *m*-H)
					13.2 (2H, d, J = 5 Hz, *m*-H)
					11.7 (2H, t, J = 8 Hz, *p*-H)
[U{OC(Me)$_2$CH$_2$SiMe$_3$}$_2$}{HB(pz)$_3$}$_2$] (**10**)				−13.6	15.9 (12H, Me)
					16.1 (4H, CH$_2$)
				(2H)	3.3 (18H)
[UCl{OC(Me)$_2$CH$_2$C(=O)Me}{HB(pz)$_3$}$_2$] (**11**)	26.7	6.5	−0.2	−17.9	75.3 (2H, CH$_2$)
					70.9 (6H, Me)
	(6H)	(6H)	(6H)	(2H)	15.8 (3H, Me)
[UCl{OC(Me)$_2$CH$_2$SiMe$_3$}{HB(pz)$_3$}$_2$] (**12**)	27.1	6.5	−0.2	−18.0	76.5 (2H, CH$_2$)
					72.5 (6H, Me)
	(6H)	(6H)	(6H)	(2H)	16.4 (9H, Me)

[a] The chemical shifts are in ppm from TMS; downfield shifts are positive; s = singlet, t = triplet; d = doublet; all the spectra were run in toluene-d_8.

tion of the mixed compound [U(CH$_2$Ph)(OEt){HB(pz)$_3$}$_2$] was undertaken to verify if the reduction of the uranium could be prevented. As the ^{1}H NMR was very different from the usual in this family of complexes, we tried to verify what will happen with analogous compounds with other alkyl groups, which do not promote reduction.] This trend is very significant for the protons of the carbon directly coordinated to the metal and is attenuated for the protons which are farthest from the uranium. Considering [U(Me)(OEt){HB(pz)$_3$}$_2$] and [UCl(Me){HB(pz)$_3$}$_2$] we found $\Delta\delta \cong 338$ ppm for the protons of the methyl groups, and this value is comparable to the one found for the *CH*$_2$ protons in [UCl(CH$_2$SiMe$_3$){HB(pz)$_3$}$_2$] and [U(CH$_2$SiMe$_3$)(OEt){HB(pz)$_3$}$_2$]. For the benzyl derivative we did not stabilize the chloride complex, but the chemical shift of the *CH*$_2$ protons in [U(CH$_2$Ph)(OEt){HB(pz)$_3$}$_2$] compares to the values found in the other mixed complexes. It is generally accepted that the large paramagnetic chemical shifts in uranium complexes reflect, in general, both dipolar and contact effects [53]. The relative contribution of these effects would probably help in the understanding of the above described results. However, the low symmetry of this family of eight-coordinate compounds as well as their fluxional behaviour in solution do not allow such type of analysis.

In **4** the bulkiness of the hydrocarbyl C$_6$H$_4$-*o*-CH$_2$NMe$_2$ and the large steric crowding around the uranium is responsible for the pattern of the ^{1}H NMR spectrum at 300 K: three broad resonances at −15.9 (6H), 30.8 (2H) and −5.6 ppm (2H) due to *NMe*$_2$, *CH*$_2$, and *B–H* protons respectively. This spectrum was indicative of a dynamic process slow in the ^{1}H NMR time scale [50]. By lowering the temperature a static spectrum at 220 K was obtained which was compatible with the C_1 symmetry expected for **4**: 20 resonances for the protons of the poly(pyrazoly)borate ligands, two resonances for the *NMe*$_2$ group, two resonances for the diastereotopic *CH*$_2$ protons, and four resonances for the protons of the phenyl ring (see Section 2). From the splitting of the *B–H* protons of the {HB(pz)$_3$} ligands, the activation energy for the dynamic process normally presented by the compounds containing the moiety 'U{HB(pz)$_3$}$_2$' was calculated at the coalescence temperature to be $\Delta G^{\neq} = 48 \pm 2$ kJ mol^{-1} (*(B–H)* protons: $\delta_1 = -3.98 \times 10^3\,T^{-1} + 9.73$; $\delta_2 = -7.90 \times 10^3\,T^{-1} + 8.94$, $T_c = 270$ K, $\Delta\nu = 1466$ Hz) [54]. The resonances of the methyl groups of the alkyl ligand, which are magnetically equivalent at room temperature, coalesce at 275 K and give rise to two signals in a 1:1 intensity ratio, which follow an approximate Curie relationship. Based on these two resonances and by extrapolation of the data we found at the coalescence temperature $\Delta G^{\neq} = 46 \pm 3$ kJ mol^{-1} ($T_c = 275$ K, $\Delta\nu = 1205$ Hz, $\delta_1 = -0.41 \times 10^3\,T^{-1} - 7.88$; $\delta_2 = -14.30 \times 10^3\,T^{-1} + 25.42$). The similarity of the $\Delta G^{\neq}$ calculated by the standard coalescence point formalism from the coalescence of the methyl groups of the *NMe*$_2$ or of the protons coordinated to the boron suggests that we are probably dealing with the same dynamic process. The *o*-(dimethylamine)methylphenyl ligand can chelate to the metal centre with formation of a five-membered metallocyclic ring [55–57]. Assuming such a

bond in **4**, in solution a breaking of the U–N donor bond, followed by rotation around the CH_2–NMe_2 axis and a remaking of the U–N donor bond could be responsible for the magnetic equivalence at 300 K of the two diastereotopic methyl groups and methylenic protons. As discussed in this work for the aldolate derivative (see above), the formation of a U–N donor bond is unexpected in this family of complexes. So, restricted rotation of the alkyl group and interconversion of the common eight-coordinate polyhedra (SAP, DD, BCTP) may be responsible for the solution behaviour [50]. When this process is fast on the ^{1}H NMR time scale the splitting observed for the protons of the poly(pyrazolyl)borate ligands shows an apparent high symmetry, and that can probably also account for the equivalence of the diastereotopic groups of the alkyl. When a static spectrum is obtained we have for the protons of the pyrazolyl ligands a pattern consistent with a C_1 symmetry, with no symmetry plane passing through the nitrogen and carbon atoms of the alkyl group. Further evidence for considering this process is the value of the activation energy found, that can be compared with the $\Delta G^*(T_c)$ values for identical processes in complexes of the type $[UClX\{HB(pz)_3\}_2]$ (X = NEt_2; 3,5-Me_2pz; 2,4,6-$Me_3OC_6H_2$) [50].

As can be seen in Table 5, for **7** and **8** only two resonances were observed for the protons of the pyrazolate ligands. For these compounds variable temperature ^{1}H NMR studies indicate that the line shape of the resonances due to the protons of the poly(pyrazolyl)borate ligands is temperature independent and the chemical shifts follow an approximate Curie relationship. However, the resonances due to the protons of the pyrazolate ligands broaden and collapse, and for **8** it was possible to observe the splitting of the resonance attributed to the H(3) and H(5) into two resonances of equal intensity. This was indicative of fluxional behaviour and the activation energy at the coalescence temperature was $\Delta G^* = 42 \pm 3\,kJ\,mol^{-1}$. This process may not be related to interconversion between eight-coordinate polyhedra, as we did not observe any alteration in the pattern of the protons of the poly(pyrazolyl)borates. We think that it can be related either with hindered rotation of the pyrazolate ligands or with an intramolecular exchange process between the two nitrogen atoms. The activation energy for this process must be lower for the less congested complex **7**, so no static spectrum could be obtained. Based on the static spectrum we cannot say if the pyrazolate ligands in **8** are mono- or bidentate, as the splitting for the protons of these ligands would be the same in any of these situations. We must mention that X-ray crystallographic analysis for $[U(pz)_2(C_5Me_5)_2]$ and $[UCl(pz)(C_5Me_5)_2]$ indicated a bidentate coordination for the pyrazolate ligands [41]. For **9** the pattern of the spectrum did not change with the temperature, indicating that the presence of the OMe group in the *ortho* position did not slow down the dynamic process normally presented by this family of compounds.

In compound **10** the bulkiness of the two alkoxide ligands coordinated to the uranium is also responsible for the ^{1}H NMR spectrum obtained at 300 K: only three resonances, due to the alkoxide groups at 16.1 (4H, *CH_2*), 15.9 (12H, *Me*) and at 3.3 ppm (18H, Si*Me_3*) and only one resonance at −13.6 ppm for the protons of the poly(pyrazoly)borate. The static spectrum obtained at 220 K was consistent with a C_2 symmetry: ten resonances for the protons of the $\{HB(pz)_3\}$, two resonances for the *CH_2* group, two for the *Me* groups and only one for the Si*Me_3*. Based on the splitting of the diastereotopic CH_2 and Me groups, the activation energy was found to be at the coalescence temperature $\Delta G^* = 55 \pm 7\,kJ\,mol^{-1}$ (*CH_2*: $T_c = 295$ K, $\Delta\nu = 488$ Hz, $\delta_1 = 2.55 \times 10^3\,T^{-1} + 9.81$, $\delta_2 = -1.77 \times 10^3\,T^{-1} + 6.37$; *Me*: $T_c = 283$ K, $\Delta\nu = 165$ Hz, $\delta_1 = 1.99 \times 10^3\,T^{-1} + 10.37$, $\delta_2 = 1.40 \times 10^3\,T^{-1} + 10.39$).

3.6. Solid-state and molecular structures

3.6.1. *[U(OC$_6$H$_4$-o-OMe)$_2${HB(pz)$_3$}$_2$] (9)*

The ORTEP drawing of the molecule is shown in Fig. 1 and selected bond distances and angles are listed in Table 6. The structure consists of discrete molecules in which the uranium atom is eight-coordinate in a distorted square antiprismatic (SAP) geometry (Fig. 2). Both 'square' faces, O(1)–N(2)–N(4)–N(6) and O(2)–N(1)–N(3)–N(5) are quite folded, with dihedral angles of 8.4 and 9.7°, which led to distortion of the SAP along the geometric pathway towards the dodecahedron (DD). Distorted SAP → DD geometries have been observed in a few structures of poly(pyrazolyl) complexes,

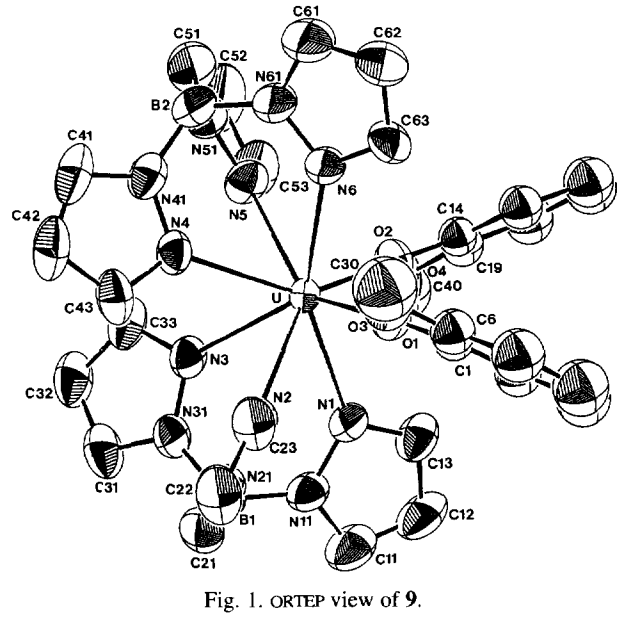

Fig. 1. ORTEP view of **9**.

$[UX_2\{HB(pz)_3\}_2]$, in which the two ligands X are similar, namely the structures of $[U(S^iPr)_2\{HB(pz)_3\}_2]$ and $[Th(OC_6H_5)_2\{HB(pz)_3\}_2]$ [17,52].

The U–O bond distances and the U–O–C bond angles are similar (2.124(6), 2.110(6) Å and 168(1), 170(1)° respectively). These very short U–O bonds and the almost linear U–O–C bond angles are comparable with the distance and bond angle previously found in $[UCl(OC_6H_5)\{HB(pz)_3\}_2]$ (2.076(12) Å, 165(1)°) [43] and provide some evidence of π-bonding between U and O. These values also compare with the U–O bond lengths and U–O–C angles found in $[UCl(O^tBu)\{HB(pz)_3\}_2]$ (2.032(5) Å, 165(1)°) [43] in $[UX(OEt)\{HB(pz)_3\}_2]$ (X = Cl, I: 2.028(9) Å, 171(1)° and 2.027(9) Å, 172(1)°) [18] and in the alkoxides $[U(BH_4)_3\{OC(^tBu)_3\}(THF)]$ (U–O, 1.97(1) Å and U–O–C 178.6(3)°) and $[U(BH_4)\{OC(^tBu)_3\}_3]$ ($U-O_{av}$ 2.07 Å and $U-O-C_{av}$ 170°) [9], in which strong π-bonding between the U and O atoms has also been suggested.

Taking into account the difference of 0.05 Å between the ionic radius of uranium(IV) and thorium(IV), a comparison with the structure of $[Th(OC_6H_5)_2\{HB(pz)_3\}_2]$ [17] shows similar An–O bond length (av. 2.177(6) Å). The Th–O–C bond angle of 171.2° is also almost linear.

The U–N bond distances range from 2.553(8) to 2.649(8) Å, with a mean value of 2.59(4) Å, in the range of values observed in the eight-coordinate poly(pyrazoly)borate uranium complexes [50].

The O–U–O bond angle of 89.4(3)° is comparable with the value of 89.6(3)° found in $[Th(OC_6H_5)_2\{HB(pz)_3\}_2]$, but is larger than the value of 86.2(5)° observed for the Cl–U–O bond angle in $[UCl(OC_6H_5)\{HB(pz)_3\}_2]$ [43], reflecting the larger size of two phenoxide ligands in **9**. In the phenoxide ligands, the terminal methoxide groups have similar $O-CH_3$ bond lengths and $C-O-CH_3$ bond angles (1.42(1) Å for O(3)–C(30), 1.40(1) Å for O(4)–C(40) and 118(1)° for C(6)–O(3)–C(30) and C(9)–O(4)–C(40)). The phenoxide rings are approximately planar, making a dihedral angle of 46.7(3)°.

The dimensions of the $\{HB(pz)_3\}$ ligands are normal and compare well with the values found in other poly(pyrazolyl)borate uranium complexes. The N–U–N angles average 71(2)°. The pyrazolyl rings are approximately planar.

Table 6
Selected bond lengths (Å) and bond angles (deg) for $[U(OC_6H_4\text{-}o\text{-}OMe)_2\{HB(pz)_3\}_2]$ (**9**)

U–O(1)	2.1246	U–O(2)	2.110(6)
U–N(1)	2.575(8)	U–N(4)	2.615(8)
U–N(2)	2.568(8)	U–N(5)	2.587(8)
U–N(3)	2.649(8)	U–N(6)	2.553(8)
O(1)–C(1)	1.345(8)	O(2)–C(14)	1.363(9)
O(3)–C(6)	1.361(10)	O(4)–C(19)	1.395(12)
O(3)–C(30)	1.423(14)	O(4)–C(40)	1.345(8)
B–N [a]	1.53(1)	C–C [a]	1.38(1)
N–N [a]	1.364(3)	N–C [a]	1.341(6)
C–C [b]	1.39(2)		
O(1)–U–O(2)	89.4(3)	N(4)–U–N(5)	72.7(3)
O(1)–U–N(1)	88.0(3)	N(4)–U–N(6)	70.1(3)
O(1)–U–N(2)	73.5(3)	N(5)–U–N(6)	71.4(3)
O(1)–U–N(4)	110.0(3)	N(1)–U–N(5)	118.4(3)
O(1)–U–N(6)	74.2(3)	N(2)–U–N(4)	73.7(3)
O(2)–U–N(1)	73.7(3)	N(2)–U–N(6)	118.2(3)
O(2)–U–N(3)	108.4(3)	N(3)–U–N(4)	72.5(3)
O(2)–U–N(5)	74.2(3)	N(3)–U–N(5)	73.5(3)
O(2)–U–N(6)	88.8(3)	U–O(1)–C(1)	168.3(4)
N(1)–U–N(2)	71.0(3)	U–O(2)–C(14)	170.0(4)
N(1)–U–N(3)	69.0(3)	C(6)–O(3)–C(30)	117.8(9)
N(2)–U–N(3)	73.5(3)	C(19)–O(4)–C(40)	117.8(8)
N–B–N [a]	109(1)	C–C–C [b]	120(2)

[a] Mean value for the pyrazolyl rings.
[b] Mean value for the phenyl rings.

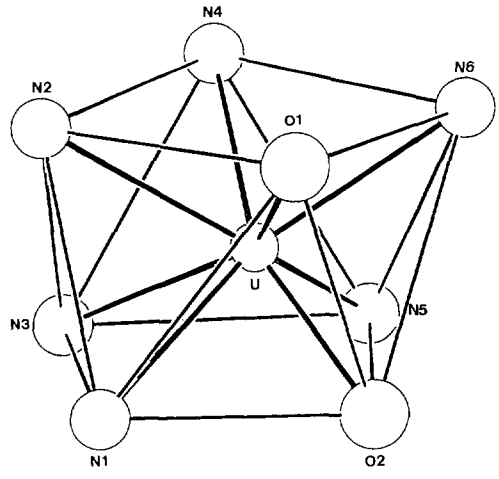

Fig. 2. SAP coordination polyhedron of **9**.

3.6.2. *[UCl(Hpz)(O^{t}Bu){(μ-O)B(μ-pz)(pz)$_2$}]$_2$* (**13**)

The structure consists of centrosymmetric dimers, in which the U_2O_2 ring is planar with asymmetrically bridging oxygen atoms. The polypyrazolylborate ligand (in which the hydrogen was replaced by an oxygen) is bidentate, with the uncoordinated pyrazole group bridging the symmetrically equivalent uranium atom. The uranium atoms are separated by 3.937(1) Å.

Fig. 3 shows an ORTEP drawing of the dimer and Table 7 shows selected bond distances and angles. The uranium atom is eight-coordinate and displays distorted dodecahedral geometry (DD), as shown in Fig. 4. In terms of a regular MA_4B_4 dodecahedron, the N(1), N(2), N(3)′ and O(1)′ atoms occupy the A sites while the N(4), Cl, O(2) and O(1) atoms occupy the B sites. The DD geometry may be characterized by two orthogonal A_2B_2 trapezoidal planes (the ϕ values for the

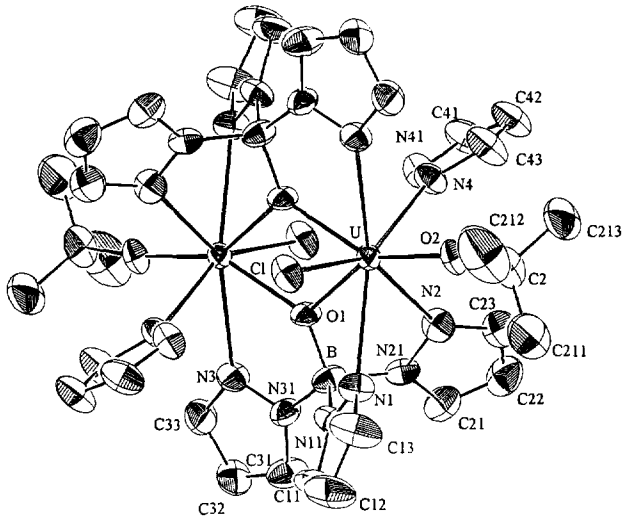

Fig. 3. ORTEP view of **13**.

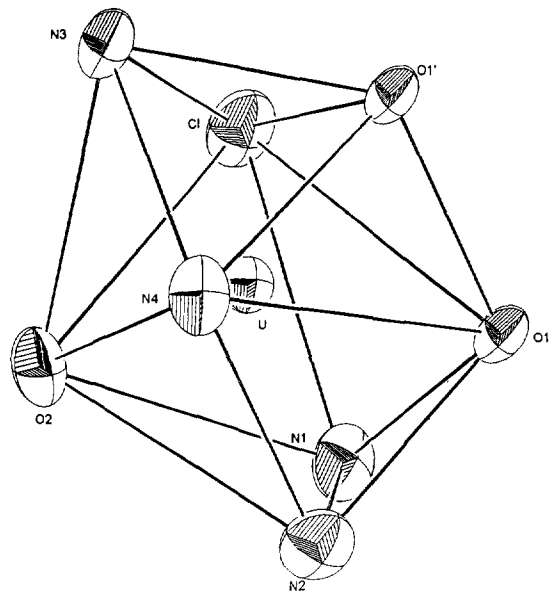

Fig. 4. DD coordination polyhedron of **13**.

planarity of the two orthogonal trapezoids average 1.2°, compared with zero for a regular DD polyhedron) [58]. Least-squares calculations on the U, N(4), Cl, N(1), N(2) plane show the large displacement of 0.016 Å from the plane for the N(2) atom, while for the plane U, O(2), N(3)′, O(1)′, O(1), the largest displacements from the plane are 0.063 and 0.040 Å for U and O(2) atoms respectively. Significant distortions from the idealized geometry are observed, mainly due to the geometric constraints imposed by the dimeric nature of the structure (short intramolecular distances of 2.463 and 2.647 Å for O(1) · · · O(1)′ and O(1) · · · N(3) respectively) and also due to the steric hindrance imposed by the different ligands around the metal centre.

Table 7
Selected bond lengths (Å) and bond angles (deg) for $[UCl(Hpz)(O^tBu)(\mu\text{-}O)B(\mu\text{-}pz)(pz)_2]_2$ (**13**)

U–Cl	2.740(3)	N(41)–C(41)	1.33(2)
U–O(1)	2.355(8)	C(41)–C(42)	1.37(2)
U–O(1)′	2.290(9)	C(42)–C(43)	1.38(2)
U–O(2)	2.045(9)	O(2)–C(2)	1.45(2)
U–N(1)	2.663(10)	C(2)–C(211)	1.45(3)
U–N(2)	2.615(11)	C(2)–C(212)	1.47(3)
U–N(3)	2.597(10)	C(2)–C(213)	1.49(2)
U–N(4)	2.581(10)	C–C [a]	1.37(3)
O(1)–B	1.41(2)	N–C [a]	1.34(3)
N(4)–N(41)	1.32(2)	N–N [a]	1.36(2)
N(4)–C(43)	1.34(2)	B–N [a]	1.54(2)
Cl–U–O(1)	99.0(2)	O(1)′–U–N(3)′	65.2(3)
Cl–U–O(1)′	84.9(3)	O′(1)–U–N(4)′	78.6(4)
Cl–U–O(2)	93.0(3)	O(2)–U–N(1)	89.2(4)
Cl–U–N(1)	72.1(3)	O(2)–U–N(2)	87.1(4)
Cl–U–N(2)	141.8(2)	O(2)–U–N(3)′	83.1(4)
Cl–U–N(3)	76.9(3)	O(2)–U–N(4)	87.7(4)
Cl–U–N(4)	149.4(3)	N(1)–U–N(2)	69.8(4)
O(1)–U–O(1)′	64.1(3)	N(1)–U–N(3)′	147.5(4)
O(1)–U–O(2)	147.2(3)	N(1)–U–N(4)	138.6(4)
O(1)–U–N(1)	66.1(3)	N(2)–U–N(3)′	140.7(4)
O(1)–U–N(2)	64.9(3)	N(2)–U–N(4)	68.8(4)
O(1)–U–N(3)′	129.3(3)	N(3)′–U–N(4)	72.8(4)
O(1)–U–N(4)	96.7(3)	B–O(1)–U	114.9(8)
O(1)′–U–O(2)	147.9(3)	B–O(1)–U′	129.0(8)
O(1)′–U–N(1)	120.0(3)	U–O(2)–C(2)	169.8(9)
O(1)′–U–N(2)	113.9(4)	N–B–N [a]	110(3)

[a] Mean value for the pyrazolyl rings.
[b] The prime label refers to the symmetry equivalent atom at $-x+1,-y,-z$.

In the U_2O_2 ring, the U–O bond distance is slightly longer than the U–O′ distance (2.355(8) and 2.290(9) Å respectively). The U–Cl bond distance of 2.740(3) Å is at the high end of the range found in previously determined eight-coordinate polypyrazolylborate uranium complexes (range: av. 2.628(8)–2.697(2) Å in $[UCl_2\{HB(pz)_3\}_2]$ and $[UCl(O^tBu)\{HB(pz)_3\}_2]$) [50], certainly due to the large steric requirement imposed by the dimeric nature of the compound.

The U–N bond distance ranges from 2.60(1) to 2.66(1) Å, with a mean value of 2.62(1) Å, slightly longer than the value of 2.58(1) Å found in the U–N(4) bond length of the coordinate pyrazole.

The closest analogy is the dimeric structure of $[UCl\{H(\mu\text{-}H)B(3,5\text{-}Me_2pz)_2\}\{H(\mu\text{-}O)B(3,5\text{-}Me_2pz)_2\}]_2$ [30], formed during the recrystallization of $[UCl_2\{H_2B(3,5\text{-}Me_2pz)_2\}_2]$ [30] in which a $(UO)_2$ ring is also present. The coordination geometry at each uranium is described as SAP → DD. As expected the O–U–O′ and U–O–U′ angles observed in this structure are respectively greater and smaller than the corresponding values observed in **13** (66.5(2) and 113.4(2)° compared with 64.1(3) and 116.0(3)°). The molecular structure of **13** is rather unusual since the bridging pyrazole group of the ligand appears to be structurally unprecedented among structures involving the $\{HB(pz)_3\}$ ligand.

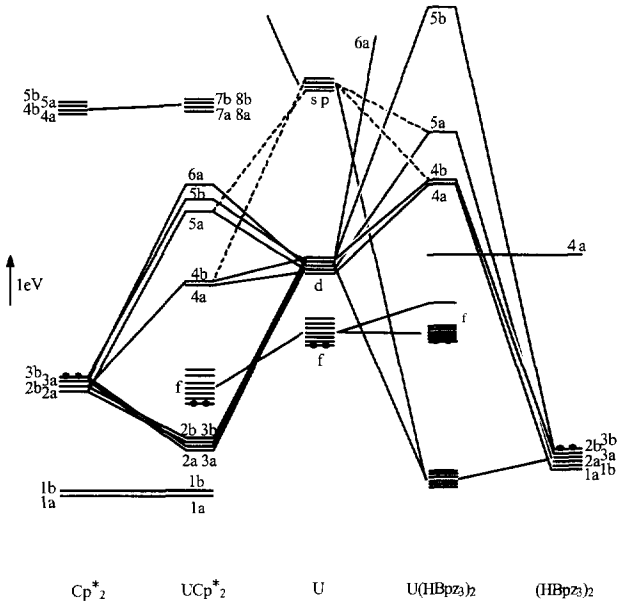

Fig. 5. Interaction diagram for the ML_2 fragment.

3.7. Molecular orbital calculations

A different behaviour in the stabilization of hydrocarbyls containing the moieties '$[U\{HB(pz)_3\}_2]$' or '$[U(C_5Me_5)_2]$' has been experimentally observed and discussed in detail above. In order to understand the stereochemical and electronic differences between these two ligands, extended Hückel MO calculations were carried out and the bonding of these two types of ligands to an actinide metal centre was studied.

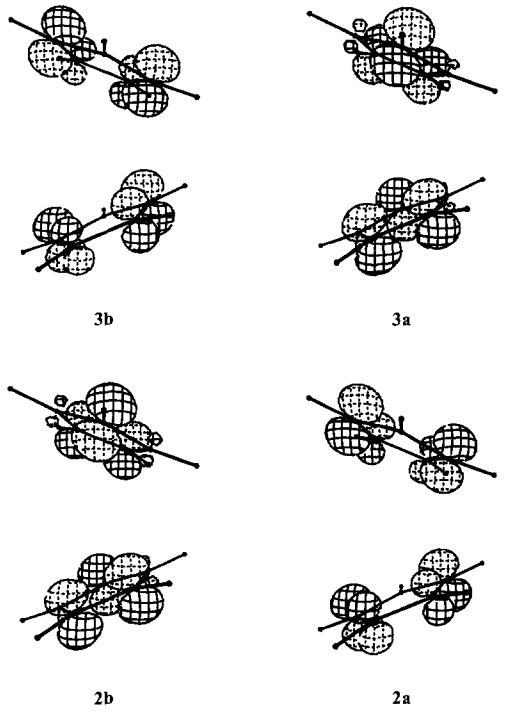

Fig. 6. Occupied frontier orbitals of the Cp_2^* fragment.

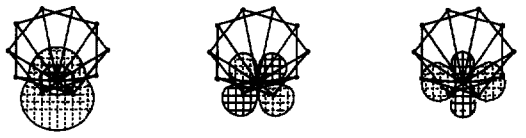

Fig. 7. Frontier orbitals for the MCp_2^* fragment.

The diagram of Fig. 5 represents how two bent Cp^* rings (left) or two bent $HB(pz)_3$ ligands (right) interact with one uranium atom. It can be seen that the Cp^* is a better stabilizing ligand, as it gives rise to lower energy molecular orbitals. The most important metal–ligand interaction involves the symmetric and antisymmetric combinations of Cp^* e_1 p orbitals (**2a**, **2b**, **3a** and **3b**, Fig. 6) and their higher energy relative to that of the corresponding orbitals of the $HB(pz)_3$ allows stronger interaction with the high energy d and f orbitals of the metal centre.

When the ML_2 (L = Cp^* or $HB(pz)_3$) fragment acts as an acceptor toward incoming ligands, it uses essentially the **4a**, **4b** and **5a** frontier orbitals (Fig. 7) which are mainly d in character. Though f orbitals will mix, their contribution to bonding is very small, in spite of being unoccupied, owing to their contracted nature.

In the $U\{HB(pz)_3\}_2$ fragment these three acceptor orbitals are not the lowest unoccupied orbitals even when f orbitals are not considered. The LUMO, represented in the diagram (Fig. 5), is essentially located in the $HB(pz)_3$ ligands, so that nucleophilic reagents are liable to attack them, making reaction at the metal centre more difficult. The consequence will be the decomposition of the $HB(pz)_3$ ligand, which is a well documented process. On the other hand, the LUMOs of the UCp_2^* fragment have lower energy than the $U\{HB(pz)_3\}_2$ analogues, giving rise to stronger interactions with any incoming ligand and there is no similar competing reaction.

These two factors, better stabilizing effect of the Cp^* ligand and lower energy LUMOs of the UCp_2^* moiety, explain the differences in stability of the $[UCp_2^*R_2]$ complexes when compared with the $[U\{HB(pz)_3\}_2R_2]$ analogues.

A second question we want to address is the stability of the hydrocarbyls described in this work compared to

Table 8
HOMOs, their character and overlap populations with orbitals of $[U\{HB(pz)_3\}_2]$ for several R groups in complexes $[UClR\{HB(pz)_3\}_2]$

R Group	HOMO energy (eV)	% z Character	OP
CH_3	−11.75	95	0.37
CH_2SiMe_3	−11.37	80	0.30
CH_2Ph	−11.24	57	0.24
$CH_2C_6H_4NMe_2$	−11.15	55	0.23
CH_2CMe_3	−11.06	82	0.33

the variation in the metal–alkyl bond disruption enthalpies experimentally determined for them in some families of compounds. The R groups studied were, respectively, CH_3, CH_2SiMe_3, CH_2Ph, $CH_2C_6H_4NMe_2$, and CH_2CMe_3. We calculated for each of them the energy of the donor orbital, the HOMO. In principle, the higher the energy, the stronger the interaction with the orbitals of $[U\{HB(pz)_3\}_2]$ will be, on energy grounds. In order to get an indication about the influence of overlap and considering that the metal fragment is always the same, we calculated the overlap population between the HOMO and every metal orbital with which it can overlap in a complex $[U\{HB(pz)_3\}_2RCl]$. The p_z character of the HOMO is also given, as a measure of the directionality of the orbital, z being the U–C axis. These results are collected in Table 8.

As discussed earlier, only the derivatives of CH_3 and CH_2SiMe_3 were experimentally obtained. The results in Table 8 indicate that the best donors (higher energy HOMO) should interact more strongly, but these are exactly the groups which have not reacted for this system. The overlap is much better for both CH_3, CH_2SiMe_3, and CH_2CMe_3 than for the other two groups, suggesting that this factor is the dominant one and that the neopentyl derivative should be obtained if electronic effects only are considered. Though it is difficult to quantify, the problem here should be a steric one.

4. Concluding remarks

Using $[UCl_2\{HB(pz)_3\}_2]$ (**1**) as starting material it was possible to stabilize some chloro and bishydrocarbyl derivatives, but in some reactions U(III) or uncharacterizable species were formed. The difference found in the stabilization of hydrocarbyls containing the moieties '$[U\{HB(pz)_3\}_2]$' or '$[U(C_5Me_5)_2]$' may be related with the different stabilizing effect of these ligands, as well as with the energy of the LUMO of these two fragments. Extended Hückel molecular orbital calculations also confirmed the vulnerability of the $\{HB(pz)_3\}$ in the fragment '$[U\{HB(pz)_3\}_2]$', as the low energy LUMO is essentially located in these ligands. The high reactivity and the polarity of the metal carbon σ bond was confirmed in reactions with protic substrates and with acetone, which allowed the synthesis of several complexes such as alkoxides, pyrazolates and aldolates. X-ray crystallographic analysis indicates, as usual, eight-coordination for the uranium, but as the steric bulk around the metal increases the coordination geometry is on the geometric pathway from SAP to DD.

Table 9
Exponents and parameters for uranium

Orbital	$-H_{ii}$ (eV)	ξ_1	ξ_2	C_1	C_2
U 7s	5.5	1.914			
U 7p	5.5	1.914			
U 6p	30.03	4.033			
U 6d	9.19	2.581	1.207	0.7608	0.4126
U 5f	10.62	4.943	2.106	0.7844	0.3908

Acknowledgements

M.P.C. Campello is grateful to JNICT for a PhD grant.

Appendix A

All calculations were of the extended Hückel [59] type with modified H_{ij}s [60]. The basis set for the metal atoms consisted of ns, np, $(n-1)$p, $(n-1)$d, and $(n-2)$f orbitals. The s and p orbitals were described by single Slater type wave functions, and d and f orbitals were taken as contracted linear combinations of two Slater type wave functions. Only s and p orbitals were used for Cl and Si.

The geometries of the $HBpz_3$ fragment were modelled with a perfect C_{3v} symmetry. The pyrazole and Cp^* rings were taken as regular pentagons. The $(HBpz_3)_2$, Cp^*_2, $M(HBpz_3)_2$ and MCp^*_2 fragments were kept in a C_2 symmetry. The distances (pm) used are as follows: U–N 255; N–N, N–C and C–C in pz rings 138; B–H 120; C–H 108; C–C in Cp^* rings 140; and C–Me (Cp^*) 150. In the MClR fragment: U–Cl 265; U–C 245; C–C 150; C–Ph 145; Si–C 185; C–N 147; and C–C (Ph) 140.

Standard parameters were used for C, H, N, Cl and Si, while those for the uranium atom were obtained by using a semi-relativistic approach (Table 9) [59].

References

[1] R.D. Ernst, W.J. Kennelly, C.S. Day, V.W. Day, T.J. Marks, J. Am. Chem. Soc. 101 (1979) 2656.
[2] A. Zalkin, J.G. Brennan, R.A. Andersen, Acta Crystallogr. C43 (1987) 418, 421.
[3] J.M. Manriquez, P.J. Fagan, T.J. Marks, J. Am. Chem. Soc. 100 (1978) 3939.
[4] J.C. Green, O. Watts, J. Organomet. Chem. 153 (1978) C40.
[5] P.B. Hitchcock, M.F. Lappert, A. Singh, R.G. Taylor, A. Brown, J. Chem. Soc., Chem. Commun. 561 (1983); P.C. Blake, M.F. Lappert, R.G. Taylor, J.L. Atwood, W.E. Hunter, H. Zhang, J. Chem. Soc., Dalton Trans. (1995) 3335.
[6] A.M. Seyam, G.A. Eddein, Inorg. Nucl. Chem. Lett. 13 (1977) 115.
[7] P. Gradoz, D. Baudry, M. Ephritikhine, M. Lance, M. Nierlich, J. Vigner, J. Organomet. Chem. 466 (1994) 107.
[8] D. Baudry, M. Ephritikhine, W. Klaui, M. Lance, M. Nierlich,

J. Vigner, Inorg. Chem. 30 (1991) 2333.
[9] C. Baudin, D. Baudry, M. Ephritikhine, M. Lance, A. Navaza, M. Nierlich, J. Vigner, J. Organomet. Chem. 415 (1991) 59.
[10] D.L. Clark, S.K. Grumbine, B.L. Scott, J.G. Watkin, Organometallics 15 (1996) 949.
[11] P.J. Fagan, J.M. Manriquez, E.A. Maatta, A.M. Seyam, T.J. Marks, J. Am. Chem. Soc. 103 (1981) 6650.
[12] T.J. Marks, V.W. Day, in T.J. Marks, I. Fragala (Eds.), Fundamental and Technological Aspects of Organo-f-Element Chemistry, Reidel, Dordrecht, 1985, p. 115 and references cited therein; T.J. Marks, Acc. Chem. Res. 25 (1992) 57; M. Ephritikhine, New J. Chem. 16 (1992) 451; D.L. Clark, A.F. Sattelberger, in R. Bruce King (Ed.), Encyclopedia of Inorganic Chemistry, vol. 1, 1994, p. 19.
[13] S. Trofimenko, Progr. Inorg. Chem. 34 (1986) 115 and references cited therein; Chem. Rev. 93 (1993) 943 and references cited therein.
[14] N. Kitajima, W.B. Tolman, Progr. Inorg. Chem. 43 (1995) 419 and references cited therein.
[15] K.W. Bagnall, J. Edwards, J.G.H. du Preez, R.F. Warren, J. Chem. Soc., Dalton Trans. 140 (1975); I. Santos, J. Marçalo, N. Marques, A. Pires de Matos, Inorg. Chim. Acta 134 (1987) 315; A. Domingos, J. Marçalo, I. Santos, A. Pires de Matos, Polyhedron 9 (1990) 1645.
[16] I. Santos, A. Pires de Matos, First Int. Conf. on f-Elements, Leuven, 1990.
[17] A. Domingos, J. Marçalo, A. Pires de Matos, Polyhedron 118 (1992) 909.
[18] M.P.C. Campello, A. Domingos, I. Santos, J. Organomet. Chem. 484 (1994) 37.
[19] M.R. Collier, M.F. Lappert, R. Pearce, J. Chem. Soc., Dalton Trans. (1973) 445.
[20] W. Wiberg, G. Wagner, G. Muller, J. Riede, J. Organomet. Chem. 24 (1970) 647.
[21] J.F. Eastham, C.G.U.S. Screttas, Patent 3534113; Chem. Abstr. 74 (1971) 3723b.
[22] M. Schlosser, J. Hartmann, Angew. Chem., Int. Ed. Engl. 12 (1973) 508.
[23] L.E. Manzer, J. Organomet. Chem. C6 (1977) 135.
[24] L.E. Manzer, J. Am. Chem. Soc. 100 (1978) 8068.
[25] G.M. Sheldrick, SHELXS-86: Program for the Solution of Crystal Structure, University of Gottingen, Germany, 1986.
[26] G.M. Sheldrick, SHELX: Crystallographic Calculation Program, University of Cambridge, UK, 1976.
[27] C.K. Fair, MOLEN, Enraf–Nonius, Delft, The Netherlands, 1990.
[28] G.M. Sheldrick, SHELXL-93: Program for Crystal Structure Refinement, University of Gottingen, Germany, 1993.
[29] D. Cohen, T.W. Carnall, J. Phys. Chem. 64 (1960) 1933; D.C. Moody, J.D. Odom, J. Inorg. Nucl. Chem. 4 (1979) 533; P. Zanella, G. Rossetto, G. De Paoli, O. Traverso, Inorg. Chim. Acta 44 (1980) L155; J.E. Nelson, D.L. Clark, C.J. Burns, A.P. Sattelberger, Inorg. Chem. 31 (1992) 1973; J.E. Nelson, D.L. Clark, L.R. Avens, S.G. Bott, D.L. Clark, A.P. Sattelberger, J.G. Watkin, B.D. Zwick, Inorg. Chem. 33 (1994) 2248.
[30] M.A. Carvalho, A. Domingos, P. Gaspar, N. Marques, A. Pires de Matos, I. Santos, Polyhedron 11 (1992) 1481.
[31] J.G. Brennan, R.A. Andersen, A. Zalkin, Inorg. Chem. 25 (1986) 1756.
[32] A.M.R. Fachadas, Diploma Thesis, Universidade de Lisboa, 1992.
[33] J.M. Manriquez, P.J. Fagan, T.J. Marks, S.H. Vollmer, C.S. Day, V.W. Day, J. Am. Chem. Soc. 101 (1979) 5075.
[34] A. Domingos, J. Marçalo, N. Marques, A. Galvão, A. Pires de Matos, P.C. Isolani, G. Vicentini, K. Zinner, Polyhedron 14 (1995) 3667.
[35] J.W. Bruno, T.J. Marks, L.R. Morss, J. Am. Chem. Soc. 105 (1983) 6824.
[36] J.W. Bruno, H.A. Stecher, L.R. Morss, D.C. Sonnenberger, T.J. Marks, J. Am. Chem. Soc. 108 (1986) 7275.
[37] D.C. Sonnenberger, L.R. Morss, T.J. Marks, Organometallics 4 (1985) 352.
[38] W.J. Evans, D.J. Wink, D.R. Stanley, Inorg. Chem. 21 (1982) 2565; L. Amaude, G. Folcher, H. Marquet-Ellis, E. Klahne, K. Yunlu, R.D. Fischer, Organometallics 2 (1983) 344; P.C. Blake, E. Hey, M.F. Lappert, J.L. Atwood, H. Zhang, J. Organomet. Chem. 353 (1988) 307; S.W. Hall, J.C. Huffman, M.M. Miller, L.R. Avens, C.J. Burns, D.S.J. Arney, A.F. England, A.P. Sattelberger, Organometallics 12 (1993) 752.
[39] J. Marçalo, A. Pires de Matos, Polyhedron 8 (1989) 2431.
[40] B. Delavaux-Nicot, M. Ephritikhine, J. Organomet. Chem. 399 (1990) 77.
[41] C.W. Eigenbrot Jr., K.N. Raymond, Inorg. Chem. 21 (1982) 2653.
[42] J.P. Leal, N. Marques, A. Pires de Matos, M.J. Calhorda, A. Galvão, J.A. Martinho Simões, Organometallics 11 (1992) 1632.
[43] A. Domingos, A. Pires de Matos, I. Santos, J. Less-Common Met. 149 (1989) 279.
[44] I. Santos, J. Marçalo, N. Marques, A. Pires de Matos, Inorg. Chim. Acta 134 (1987) 315.
[45] H. Yasuda, K. Tatsumi, A. Nakamura, Acc. Chem. Res. 18 (1985) 120; S.L. Buchwald, B.T. Watson, J. Am. Chem. Soc. 109 (1987) 2544.
[46] R.S. Sternal, M. Sabat, T.J. Marks, J. Am. Chem. Soc. 109 (1987) 7920.
[47] H.J. Heeres, M. Maters, J.H. Teuben, G. Helgesson, S. Jagner, Organometallics 11 (1992) 350.
[48] A. Domingos, N. Marques, A. Pires de Matos, I. Santos, M. Silva, Organometallics 13 (1994) 654.
[49] H. Adams, N.A. Bailey, A.S. Drane, J.A. MacCleverty, Polyhedron 2 (1983) 465; H. Adams, N.A. Bailey, G. Denti, J.A. MacCleverty, J.M.A. Smith, A. Wlodarczyk, J. Chem. Soc., Dalton Trans. (1983) 2287; C.J. Jones, J.A. MacCleverty, A.S. Rothin, J. Chem. Soc., Dalton Trans. (1986) 109; M. Cano, J.V. Heras, S. Trofimenko, A. Monge, E. Gutierrez, C.J. Jones, J.A. MacCleverty, J. Chem. Soc., Dalton Trans. (1990) 3577; M. Cano, J.V. Heras, E. Santamaria, E. Pinilla, A. Monge, C.J. Jones, J.A. MacCleverty, Polyhedron 12 (1993) 1711; A. Paulo, A. Domingos, I. Santos, unpublished results, 1996.
[50] I. Santos, N. Marques, New J. Chem. 19 (1995) 551.
[51] J.P. Leal, J.A. Martinho Simões, J. Chem. Soc., Dalton Trans. (1994) 2687.
[52] I. Santos, A. Pires de Matos, Actinides '89, Tashkent, Russia, 1989; A. Domingos, A. Pires de Matos, I. Santos, Polyhedron 11 (1992) 1601.
[53] W. De W. Horrocks Jr., in G.N. La Mar, W. De W. Horrocks Jr., R.H. Holm (Eds.), NMR of Paramagnetic Molecules, Academic Press, New York, 1973, p. 127; R.D. Fischer, in T.J. Marks, R.D. Fischer (Eds.), Organometallics of the f-Elements, Reidel, Dordrecht, 1979, p. 337 and references cited therein.
[54] J. Sandstron, Dynamic NMR Spectroscopy, Academic Press, New York, 1982.
[55] A.L. Wayda, J.L. Atwood, W.E. Hunter, Organometallics 3 (1984) 939.
[56] A.L. Wayda, R.D. Rogers, Organometallics 4 (1985) 1440.
[57] M. Booij, N.H. Kiers, A. Meetsma, J.H. Teuben, W.J.J. Smeets, A.L. Spek, Organometallics 8 (1989) 2454.
[58] E.L. Muetterties, L.J. Guggenberger, J. Am. Chem. Soc. 96 (1974) 1748.
[59] R. Hoffmann, J. Chem. Phys. 39 (1963) 1397; K. Tatsumi, A. Nakamura, J. Am. Chem. Soc. 109 (1987) 3195.
[60] J.H. Ammeter, H.-B. Bürgi, J.C. Thibeault, R. Hoffmann, J. Am. Chem. Soc. 100 (1978) 3686.